



Research status of welding technology of ferritic stainless steel

Zhihai Dong¹ · Yiwen Li¹ · Boyoung Lee² · Aleksandr Babkin³ · Yunlong Chang¹

Received: 25 February 2021 / Accepted: 27 September 2021 / Published online: 9 October 2021
© The Author(s), under exclusive licence to Springer-Verlag London Ltd., part of Springer Nature 2021

Abstract

Ferritic stainless steel has been applied frequently owing to its advantages such as good thermal conductivity, low coefficient of linear expansion, good stress corrosion resistance, and no Ni. However, the welding process will cause the grain size of the weld zone and the heat-affected zone to grow seriously, resulting in a decrease in the toughness of the welded joint. The paper discusses in detail the traditional and improved welding methods of ferritic stainless steel. These improved methods can effectively reduce the grain size or increase the penetration. The process of introducing electric and magnetic pulses can compress the arc, increase the weld penetration, stir the molten pool, refine the grains, and improve the strength and toughness of the weld. The future development direction of ferritic stainless steel welding is discussed at the end of the article.

Keywords Ferritic stainless steel · Welding method · Grain refinement · Electric pulse · Magnetic pulse

1 Introduction

With the increasing development of industrial technology, the consumption of stainless steel has increased substantially. Among all stainless steel, austenitic stainless steels (ASS) are the most widely used. Still, due to the sharp increase in the price of the rare metal Ni, the application and development of austenitic stainless steels have been hindered. Compared with ASS, FSS has the advantages of no Ni, low cost, high thermal conductivity, small coefficient of linear expansion, and excellent resistance to stress corrosion cracking. It has been widely used in automobiles, nuclear power, petrochemical, and other industries [1–4]. Although FSS has beneficial properties under forging conditions, during the welding process, welded joints are prone to intergranular corrosion [5, 6], precipitation embrittlement, and other defects [7, 8], which make the welded joints difficult. Corrosion resistance and mechanical properties are affected. The main problem is that the welding thermal

cycle will cause the grain of the weld zone (WZ) and heat-affected zone (HAZ) to become coarser, resulting in a serious decrease in the toughness of the welded joint, and cannot be eliminated by heat treatment.

Among the welding processes of FSS, arc welding has become the most widely used process because of its flexibility, low production cost, and the ability to provide strong metal joints. However, the high temperature in most arc welding will promote the grain growth of WZ and HAZ, which leads to the decrease of weld toughness of FSS. According to the thickness of base metal (BM), groove welding or no groove welding can be selected, and austenitic welding wire can be used for filling. This is the use of the alloy strengthening method to adjust the chemical composition of the weld to improve the toughness of the welded joint, such as shielded metal arc welding (SMAW), gas metal arc welding (GMAW), and so on. But the disadvantages are low efficiency, many consumables, and high cost. Using autogenous welding methods, such as TIG welding, can reduce consumables, but it is only suitable for welding thin plates. With the successive application of high-efficiency TIG welding (such as A-TIG, K-TIG), plasma arc welding (PAW), laser beam welding (LAW) and electron beam welding (EBW), and other high-efficiency autogenous welding technologies, the efficiency problem of thick plate welding has been solved. However, in the autogenous welding of thick plate, the weld microstructure is mostly symmetrically

✉ Yunlong Chang
sychyl@126.com

¹ School of Material Science and Engineering, Shenyang University of Technology, Shenyang 110870, China

² School of Aerospace and Mechanical Engineering, Korea Aerospace University, Seoul 101-601, Korea

³ Institute of Mechanical Engineering, Lipetsk State Technical University, Lipetsk 398024, Russia

grown columnar crystals, and the service performance of the welded joint is often not satisfactory.

There are two ways of weld strengthening: alloy strengthening and fine-grain strengthening. Fine-grain strengthening provides a new way to improve the plastic toughness of FSS welded joints. In all welding methods, no matter which method, the grain growth can be limited by controlling the heat input, but most of the toughness will still be lost [9, 10]. To further improve the plastic toughness of the FSS welded joint, scholars have improved these methods, using improved methods such as adding chemical elements, pulse current, electromagnetic stirring, ultrasonic vibration, and hybrid welding to refine the grain size of FSS weld, improve the joint performance.

This article reviews the traditional and improved welding technology of FSS, discusses the influence of different methods on the weld appearance, microstructure, and performance of FSS, and is designed to provide new ideas for high efficiency and high-quality welding of FSS.

2 Ferritic stainless steel welding method

FSS has a wide range of welding methods, including fusion welding and pressure welding, such as gas tungsten arc welding (GTAW), EBW, LAW, resistance spot welding (RSW), friction stir welding (FSW), and some improvement methods. The following is a summary of the research status of FSS welding technology.

2.1 SMAW

SMAW is a commonly used welding method in industrial production. Silva et al. [11] used AWS E309MoL-16 as a filler material to weld FSS. As shown in Fig. 1, the grains in the HAZ grew significantly after welding. X-ray diffraction analysis confirmed a secondary phase, such as Laves phase, Chi phase, and Sigma phase. The experimental results show that the increase in grain size and precipitates in HAZ lead to the decrease of toughness. Since then, Silva et al. [12] also found that the chemical composition formed in the fusion zone (FZ) is related to the degree of dilution level between the filler metal and the base metal (BM), and the dilution increases with the increase of the welding heat input.

2.2 GMAW

GMAW is a high-efficiency and low-cost welding method. When using GMAW to weld FSS at home and abroad, the filled austenitic welding wire is often used. By introducing austenitizing elements to enlarge the $\alpha + \gamma$ two-phase zone, more austenite is formed to hinder the growth of ferrite grains [13–15]. The geometry of the MIG weld bead (weld

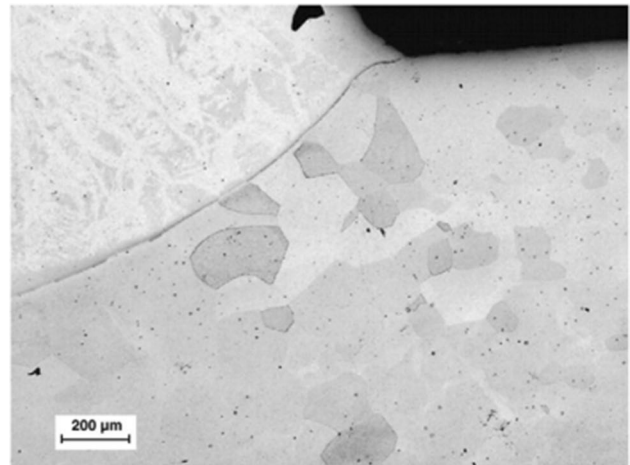


Fig. 1 HAZ microstructure of AISI 444 steel welded with 6 kJ/cm [11]

width, height of reinforcement, and depth of penetration) affects the mechanical strength of the joint. Therefore, to obtain a good welded joint, the best combination of input parameters must be determined. As shown in Fig. 2, Narang et al. [16] By studying a five-level, five-factor half-factorial design matrix based on Central composite face centered design was used for the development of mathematical models to analyze the effect of process parameters on weld bead geometry and shape relationships of MIG welded SS409L plates.

Changing the chemical composition of the filler material during MIG welding can change the microstructure of the weld, thereby improving the mechanical properties of the welded joint. For example, adding Al and Ti to the filler material can suppress the increase in weld grain size and obtain uniaxial fine grains. The hardness of the HAZ increases after welding, which is mainly caused by the acicular martensite in the HAZ, and the acicular martensite increases with the increase of heat input [17].

Although by adjusting the chemical composition of the filler material, the organization of the WZ can be improved. However, larger heat input of MIG welding will cause the heat-affected zone of the welded joint to become wider and the grain size to increase [18]. The use of pulsed GMAW (P-GMAW) can effectively limit the above problems. This method uses periodically changing pulse current for welding [19]. Since the traditional GMAW stable droplet transfer form is spray transfer, the welding current must be greater than the critical current value of the spray transfer. Otherwise, it will be globular transfer and short circuit transfer. P-GMAW can control droplet transfer and welding heat input. The study found that even under higher heat input conditions, the pulse form can produce a grain size value similar to the spray transfer, which limits the grain

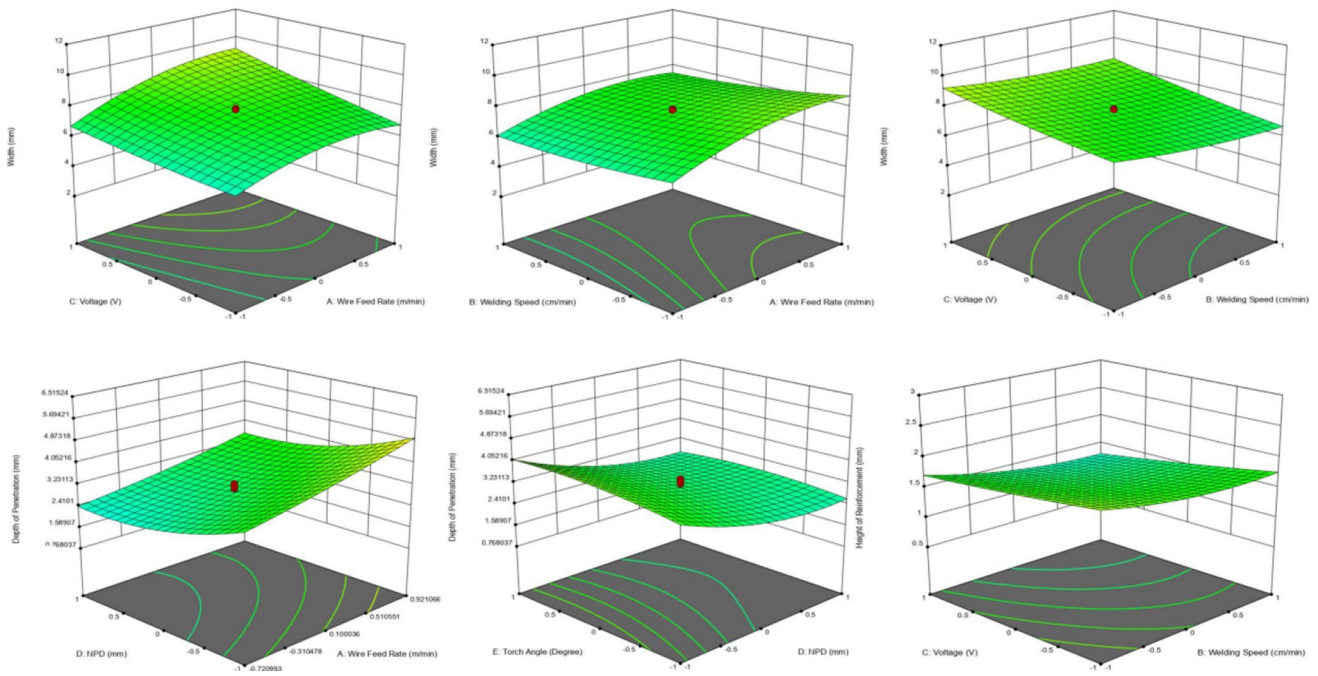


Fig. 2 Interactive effects of different welding parameters on Geometric features [16]

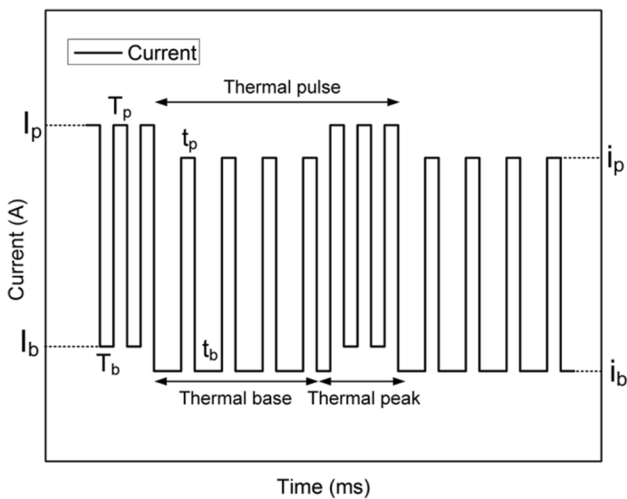


Fig. 3 Schematic of DP-GMAW waveform [20]

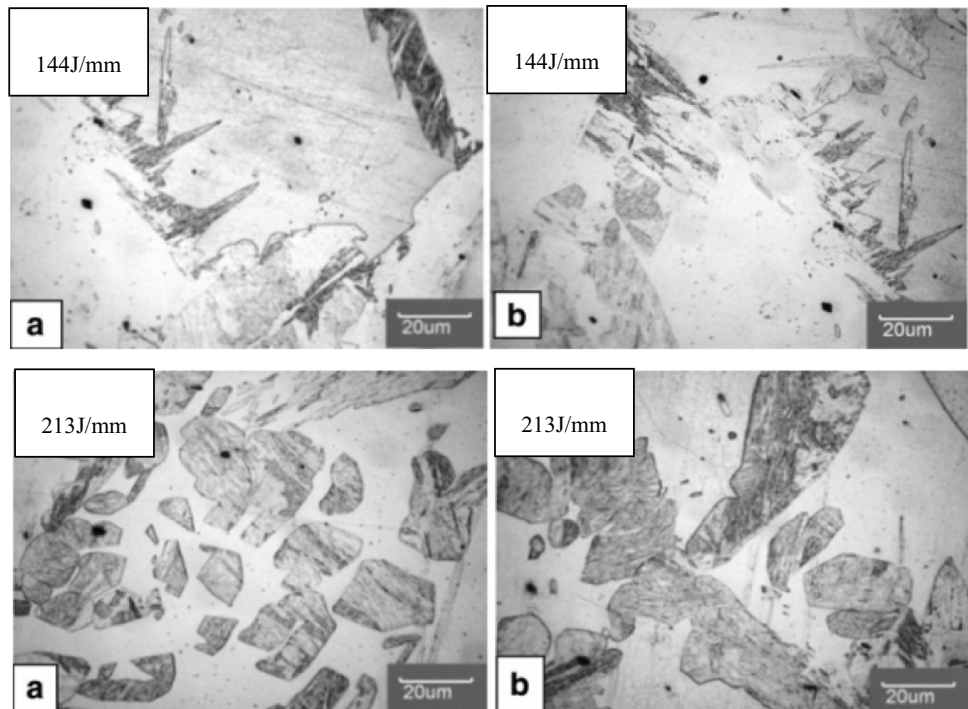
coarsening of the HAZ to a certain extent and improves the FSS welded joint of toughness.

On this basis, a double-pulse GMAW (DP-GMAW) is proposed, which can accurately control the heat input. The current waveform diagram of DP-GMAW is shown in Fig. 3. It clearly shows that a thermal pulse consists of a thermal peak period and a thermal base period. During each thermal pulse, there is a coexistence of a current pulse at a higher frequency. Obviously, both peak current value (I_p) and base current value (I_b) in the thermal peak period differ

from those (i_p and i_b) in the thermal base period, so does the pulse frequency in different thermal periods. However, the pulse duration (T_p) in the thermal peak period is kept the same as that (t_p) in the thermal base period. The thermal pulse is used to modulate the peak and duration of the higher frequency pulses to further lower heat input and to improve the fluidity of the weld pool. Moreover, the weld pool is stirred strongly by thermal pulse [20]. It has the characteristics of reducing heat input, stirring molten pool strongly, refining grain, increasing toughness, reducing porosity and crack sensitivity.

Flux Cored Arc Welding (FCAW) is a kind of welding method with gas slag combined protection. Grain coarsening is a major defect in the FCAW welding of FSS. If the heat input is not properly controlled, the grain size of HAZ near the fusion line will increase. Venkatesan et al. [21] studied the influence of FCAW process parameters on the weld for 409 m FSS. Figure 4 confirms that coarse grains occur in the HAZ of AISI409M FSS, and the martensite content increases with the increase of heat input, and the effective size of ferrite will decrease. In addition, the research results show that the change of heat input has no significant effect on the tensile properties of the joint. Therefore, it is recommended to use welding parameters that can provide uniform weld bead profile in the manufacturing process. In addition, FCAW has a certain effect on solving the problem of intergranular corrosion of FSS after welding [22]. The Ti and Nb in the flux-cored wire can form metal compounds with C and N, which reduces the precipitation of chromium carbide at

Fig. 4 Typical Photomicrograph of the ferritic heat-affected zone welded with heat input 144 J/mm, 213 J/mm microstructure a Near fusion line, b HAZ [21]



the grain boundaries, avoids the appearance of chromium-depleted areas on the grain boundaries, and improves the resistance to intergranular corrosion and pitting corrosion. As the content of Ti and Nb increases, the intergranular corrosion resistance improves.

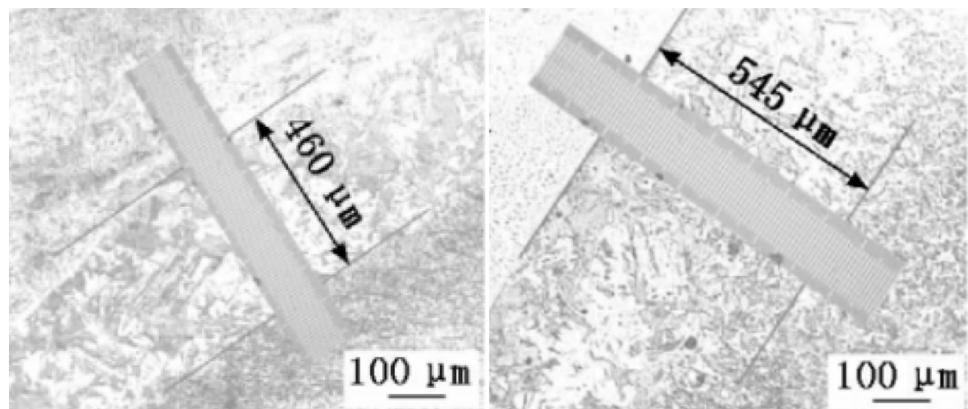
Cold Metal Transfer Welding (CMT) is a modification of GMAW. Unlike the traditional short-circuit transfer process, CMT adopts a mechanical droplet transfer form, which realizes the control of droplet transfer and low heat input. CMT can adopt the unified control mode, and the heat input can be adjusted by changing the wire feeding speed [23]. He et al. [24] used CMT to weld 4003 FSS. As shown in Fig. 5, compared with the MIG welded microstructure, CMT has a narrower coarse-grained region. The experimental results show

that the HAZ impact energy of CMT welding is 16.28% higher than that of MIG welding.

2.3 GTAW

GTAW is a high-quality welding method with the advantages of stable arc, low welding heat input, no spatter, and good welding quality [25]. Generally, the HAZ produced by GTAW welding is smaller than that of SMAW and GMAW and conforms to the rule of SMAW > GMAW > GTAW [26]. Figure 6 shows the microstructure comparison of GTAW and SMAW welded FSS. Through the analysis of the weld microstructure, it can be seen that the microstructure of the FZ of the SMAW weld is composed of dendrites, while the

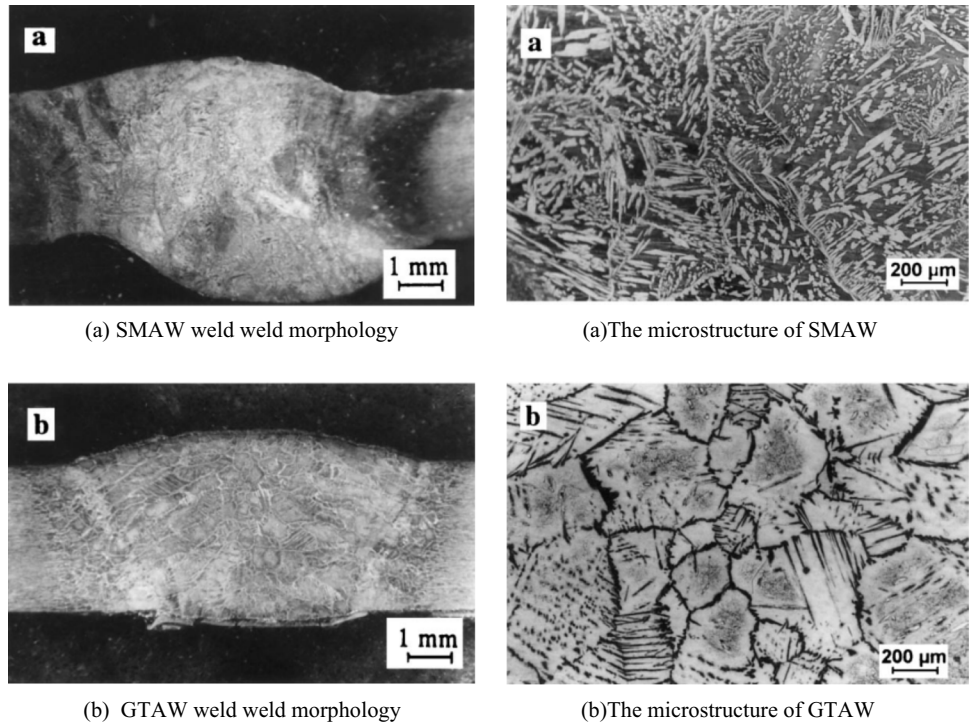
Fig. 5 Heat-affected zone microstructure [24]. (a)CMT, (b)MIG



(a) CMT

(b) MIG

Fig. 6 Weld appearances and microstructure of SMAW and GTAW [27]. (a) SMAW weld weld morphology. (b) The microstructure of GTAW. (b) GTAW weld weld morphology. (b) The microstructure of GTAW



microstructure of the FZ of the GTAW weld is dominated by fine equiaxed crystals [27]. Since the heat input is the decisive factor for grain growth [28], the heat input of GTAW welding is smaller, the HAZ is smaller, the weld microstructure is better, and it is easier to obtain an ideal FSS weld.

Mohammad et al. [29] used the autogenous TIG process to weld AISI430 FSS. They studied the temperature between weld passes (25–750 °C) on the weld microstructure and mechanical properties of the weld. As shown in Fig. 7, the research results show that when the interpass temperature is 150 °C, there are dimples in the fracture. In addition to the

main quasi-cleavage fractures, there are also some ductile fractures with the highest strength and toughness.

Amuda et al. [30] studied the effect of welding current and welding speed on microstructure and properties of medium chromium AISI 430 FSS weld during TIG welding. The study found that strict control of the welding speed can promote the production of equiaxed welds. In addition, to avoid the decrease of the microhardness of the welded joint, the heat input should be less than 15kj/mm. But according to this range to control the heat input, the grain size of the weld microstructure is still 5–8 times that of the BM. Wang et al.

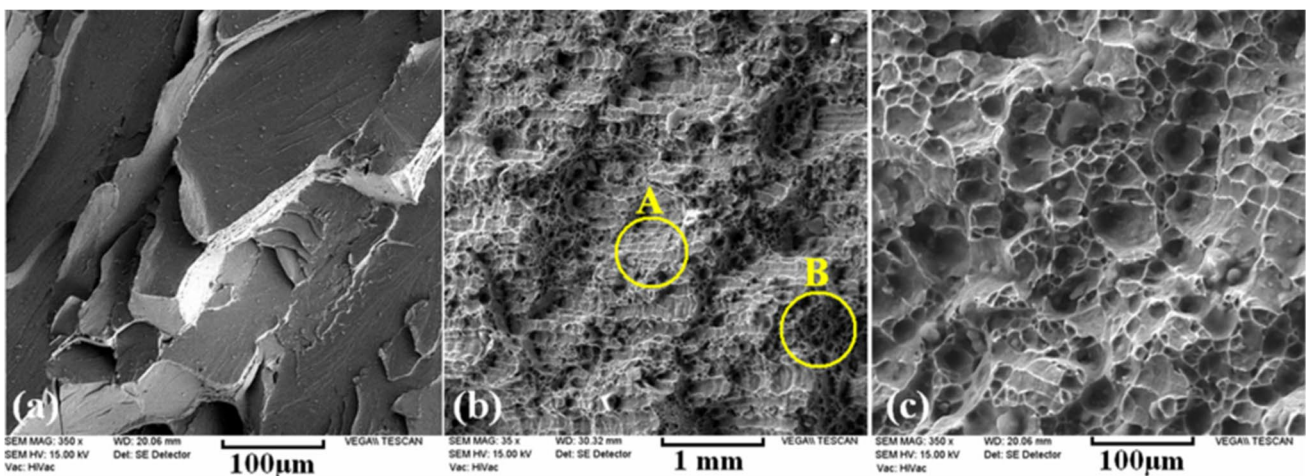


Fig. 7 The fracture surface of T150 specimen presenting (a) cleavage facets (b) quasi-cleavage fracture (c) ductile fracture by dimples [29]

[31] used numerical simulation to study the grain growth behavior in the HAZ of 443 FSS TIG welding. The study found that the grain growth in the HAZ is mainly affected by thermal cycling, grain boundary migration, and particle precipitation. Controlling the high-temperature residence time of the welding thermal cycle helps to refine grain.

Although strict control of heat input during TIG welding can get relatively ideal weld. However, due to the small current carrying capacity of the tungsten electrode, the arc energy density is not concentrated, and problems such as shallow penetration are prone to occur [32–34]. Therefore, TIG autogenous welding is only suitable for welding thin plates (below 2 mm).

To improve the penetration of TIG, researchers have improved TIG welding. Activated Flux TIG, also known as A-TIG, changes the surface tension of liquid metal through surfactant and then increases the penetration. Compared with the traditional TIG welding, the penetration of A-TIG welding can be increased by 200~300%, realizing the single pass welding of thick plate. Ramkumar et al. [35] studied A-TIG welding of AISI430 FSS. The experiment uses two different activating fluxes, SiO_2 , and Fe_2O_3 . As shown in Fig. 8, the study found that under the same welding current, the weld with activating flux achieves full penetration. The weld without activating flux does not achieve full penetration. Of welds with activating flux SiO_2 , tensile fracture occurs in the BM, and for welds with activating flux Fe_2O_3 , tensile fracture occurs in the FZ. This is due to more oxygen in the FZ of the weld with Fe_2O_3 activating flux.

Comparing the two welding methods of A-TIG and Multipass Tungsten Inert Gas Welding (M-TIG), it can be found that although A-TIG can complete single-pass welding of thick plates, the impact toughness of A-TIG welded joints are not as good as M-TIG. The reason is that the grains size of A-TIG FZ is relatively coarse, and there are manganese and oxide inclusions. Post weld heat treatment (PWHT) can improve the impact toughness of A-TIG welds [36]. In addition, the selection of A-TIG activating flux is relatively complicated, and if it is not selected properly, it may reduce the corrosion resistance of the welded joint. In literature [37] A-TIG welded joints coated with SiO_2 have better electrochemical corrosion resistance in 3.5% NaCl solution than ordinary TIG joints. However, the electrochemical corrosion resistance of joints coated with B_2O_3 , TiO_2 , and Cr_2O_3 is reduced.

Keyhole Gas Tungsten Arc Welding (K-TIG) is an improvement based on GTAW. As shown in Fig. 9, cooling water is added to the shrink nozzle of the welding torch, and a large current is used to increase the current density. Compared with the traditional TIG, the arc force is larger. During welding, the arc force can push the liquid metal of the molten pool outward to form a keyhole, and the molten pool anchors itself on the root surface of the weldment. The

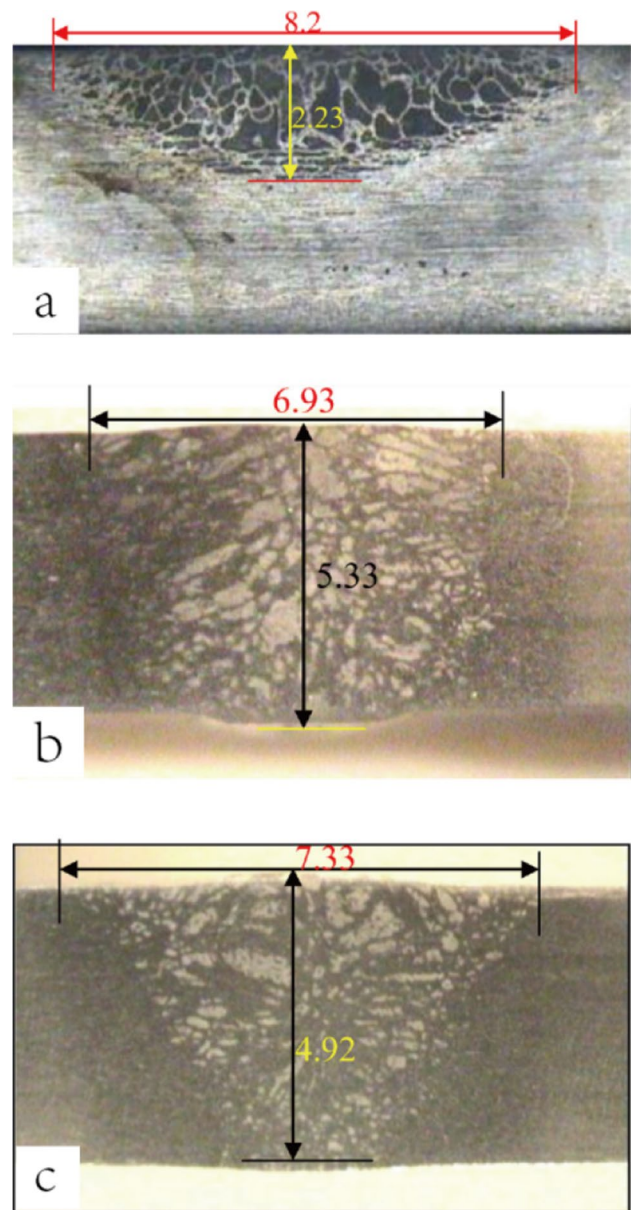
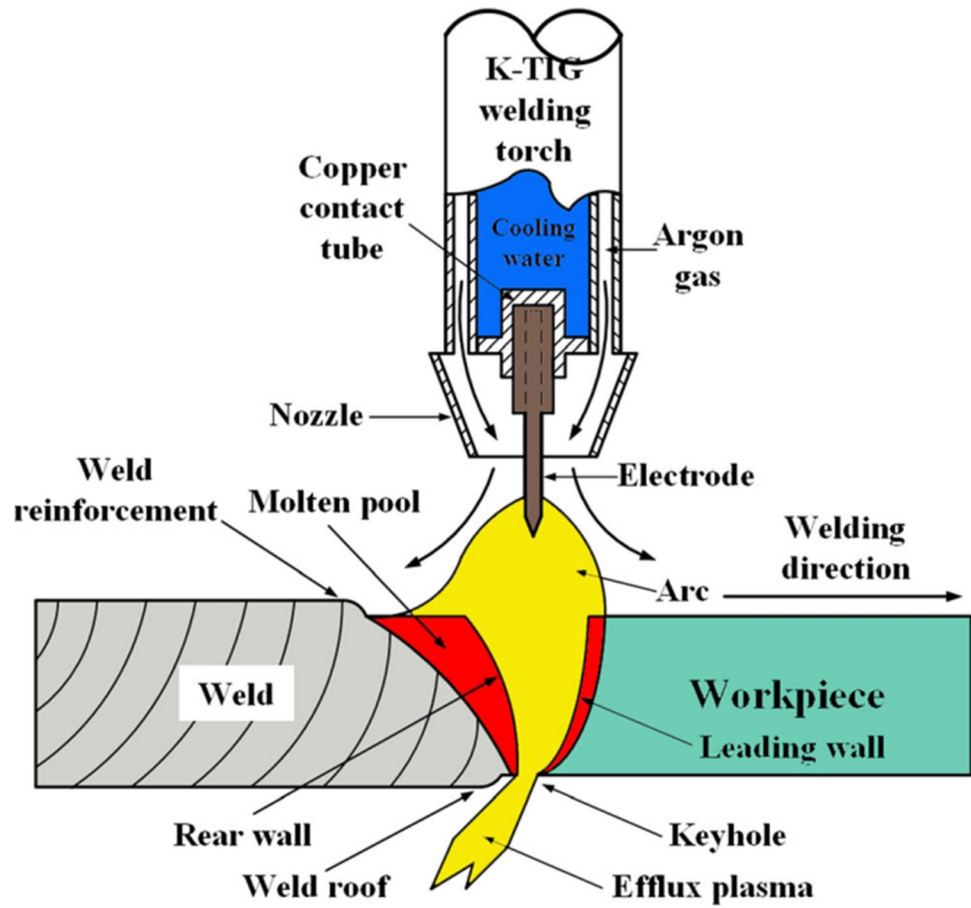


Fig. 8 Depth of penetration and bead width of autogenous TIG (a) Autogenous welding without flux (b) with SiO_2 flux and (c) with Fe_2O_3 flux [35]

arc force, liquid metal density, and surface tension are balanced to maintain the stability of the keyhole. It is a TIG welding method that can achieve a single pass deep penetration. Compared to LBW and EBW, K-TIG process has lower costs and easier operation [38, 39].

Xie et al. [40] used K-TIG to weld FSS with a one-time penetration of 8 mm. When using DC constant current K-TIG welding, the weld area is composed of columnar crystals, and the coarse crystal grains make the toughness of FSS welded joints seriously reduced. Because pulse welding has the effect of refining grains and improving mechanical

Fig. 9 Schematic of K-TIG process, the specially made torch, and the morphology of the molten pool [38]



properties [41] when using DC high-frequency K-TIG for welding, the penetration and energy density of the arc is increased, the heat input is smaller, and the weld grain size is smaller and the mechanical properties are improved.

Compared with conventional GTAW, pulsed gas tungsten arc welding (PGTAW) has many advantages, such as increasing arc energy density, reducing heat input, reducing the width of the HAZ, and increasing the depth width ratio of the weld. The pulse current has a certain effect on the instantaneous temperature and heat input during the solidification of the FSS molten pool [42, 43]. The center microstructure of the weld is composed of equiaxed crystals. Hu et al. [44] used Pulse Tungsten Inert Gas (P-TIG) to weld $\text{Cr}_{26}\text{Mo}_{3.5}$ FSS. The study found that carbides and nitrides of Ti and Nb were precipitated in the microstructure of the weld, forming insoluble particles. Insoluble particles can be used as heterogeneous nucleated particles to refine weld grains. In addition, a larger degree of undercooling and smaller temperature gradient in the molten pool is also conducive to the growth of equiaxed crystals. The precipitation of Ti and Nb carbides and nitrides in the HAZ can also hinder the growth of grains in the HAZ. Some documents point out that when high-frequency current pulse welding is used, as the pulse frequency increases, the arc shrinkage

will be more significant, the arc energy density increases, and the arc pressure increases, which can increase the penetration. In addition, the pulsed current will produce electromagnetic force in the molten pool. Under the action of larger arc pressure and electromagnetic force, the liquid metal in the molten pool will produce a complicated flow. The complex flow of liquid metal can break up columnar crystals and eventually form fine equiaxed crystals [45, 46]

Watanabe et al. [47] used Ultrasonic Assisted Tungsten Inert Gas Welding (U-TIG) to weld of FSS. Figure 10(a) shows the schematic of an apparatus for welding with ultrasonic vibration. The filler metal is ultrasonically vibrated through a guide tube attached to the top of an ultrasonically vibrating horn. Ultrasonic vibration is transmitted into the molten pool through the filler metal. The vibration direction of the welding wire is perpendicular to the surface of the paper. Figure 10(b) shows the schematic to explain the location between the filler metal and an electrode for transmitting ultrasonic vibration. Due to the physical mechanism of ultrasonic mainly include the effects of mass transfer, acoustic streaming, and cavitation [48, 49], the metal flow in the molten pool will be violent. The intense flow has an impact on the nucleation at the edge of the molten pool. In addition, violent vibration can break the growing columnar crystal,

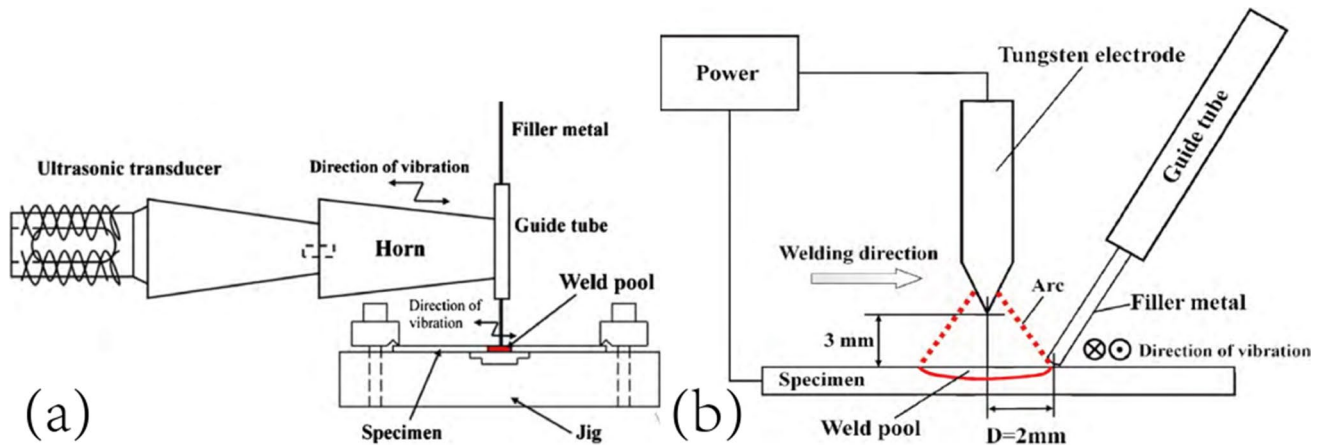


Fig. 10 (a) Schematic of an apparatus for welding with ultrasonic vibration, (b) schematic diagram of the position between the filling metal and the electrode that emits ultrasonic vibration [47]

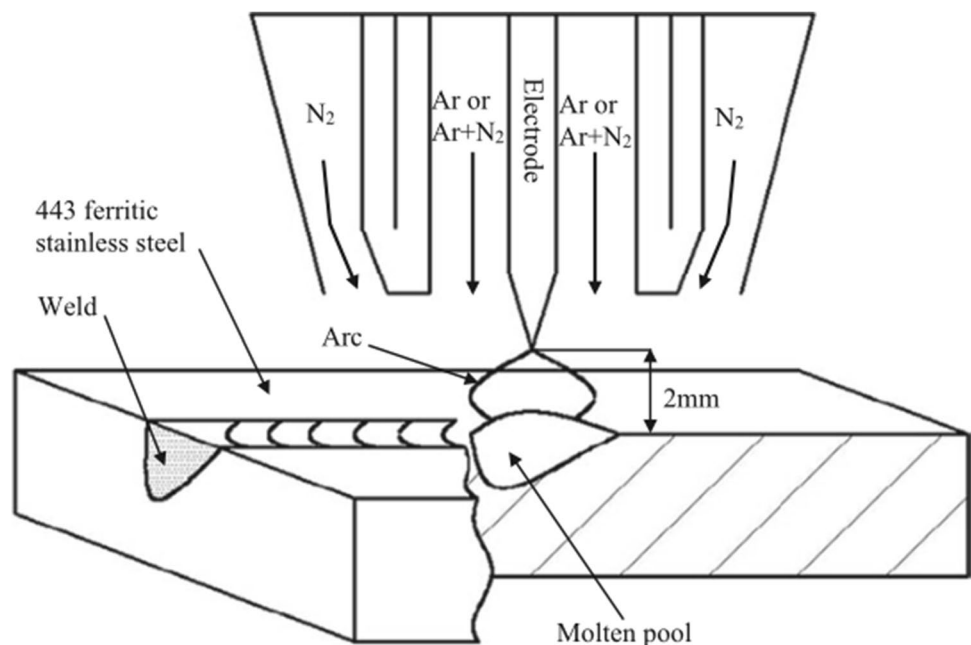
increase new nucleation particles, increase nucleation rate, and promote the transformation of columnar crystals to equiaxed crystals. They increased the tensile strength and tensile fracture elongation of FSS joints. But the disadvantage is that when the distance between an electrode tip and the filler metal was too short, the weld bead became bumpy, and two regions coexisted in the weld bead where ultrasonic vibration was transmitted or not transmitted. And not suitable for welding large components [47].

Changing the composition of the shielding gas can affect the crystallization of the molten pool. The use of Ar+N₂+O₂ mixed gas protection can refine the weld grains. The primary role of O₂ was to produce stable inoculants in the molten weld pool, in this case, Al-oxides, to enhance

TiN nucleation, which eventually nucleates equiaxed grains [50]. Although the grain size is reduced due to the increase in pore content, increase may affect impact toughness.

Some scholars have designed a welding torch with the double gas shield for welding experiments. As shown in Fig. 11, the inner layer is protected by pure Ar, and the outer layer is protected by N₂. The experimental results show that the proportion of equiaxed crystals in the microstructure of the weld increases, the grain size decreases, and the impact toughness of the HAZ increases. This is because, on the one hand, the thermal conductivity of N₂ is greater than that of Ar, and the cooling rate of welds with N₂ added is greater than that of welds without N₂, thereby increasing the cooling rate of the welds, reducing the grain

Fig. 11 Schematic diagram of GTAW torch with a gas hood during the welding process [51]



size and the width of the HAZ; On the other side, N is a stabilizer of γ , which can make the distribution of Cr and Ti more uniform and increase the strength and toughness of the welded joint [51].

Due to GTAW autogenous welding, the chemical composition of the weld cannot be adjusted by the method of filling the welding wire. Therefore, scholars use powder pre-melting technology [52], direct addition [53], and coating on the surface of the BM [54, 55], etc., to add new chemical elements to the molten pool. Chemical elements are usually added in the form of alloy powders of the same composition, heterogeneous nucleating agents and modifiers. A large amount of alloy powder of the same composition is added to the molten pool, and the molten pool produces a strong cooling effect through melting and evaporation of the alloy powder, reducing the temperature gradient to achieve the purpose of grain refinement. By adding heterogeneous nucleation alloys, high melting point stable compounds can be formed, increasing nucleation particles and promoting heterogeneous nucleation. The addition of modifiers can affect the crystal growth during the solidification process depending on the change of its morphology or performance. Since the excessive growth of grains in the molten pool during the crystallization process leads to coarse microstructure, metamorphic elements can be used to control the grain morphology, hinder the growth of dendrites during the crystallization process of the weld, and finally refine the grains. In summary, adjusting the elements of the molten pool can refine the weld microstructure of FSS. However, this method is limited to a few elements, and for the welding of different materials, it is difficult to determine the composition of the added elements. In addition, the addition of alloy elements is not uniform [51], which severely restricts the research and application of this method.

Magnetic control welding technology is an advanced welding process. The shape of the TIG arc can be controlled by the magnetic field, the stability of the arc can be improved, and the microstructure and properties of the weld can be optimized [39, 56, 57]. As shown in Fig. 12, the high-frequency magnetic field has a compressive effect on the arc. The arc pressure first presents a bimodal distribution and then a unimodal distribution with the increase of frequency, and the arc pressure increases with the increase of frequency. As shown in Fig. 13, it is found through analysis that the trajectory of the charged particles in the arc is spiral, and the spiral of the arc has a stirring effect on the molten pool. In addition, the magnetic field has a direct effect on the flow of the molten pool, and the effect of electromagnetic stirring can break the coarse columnar crystals of the weld, refine the grains, and improve the toughness of the welded joint [58]. Reddy et al. [59] used GTAW to weld AISI430 FSS and introduced external electromagnetic oscillation during the welding process. The study found that the weld

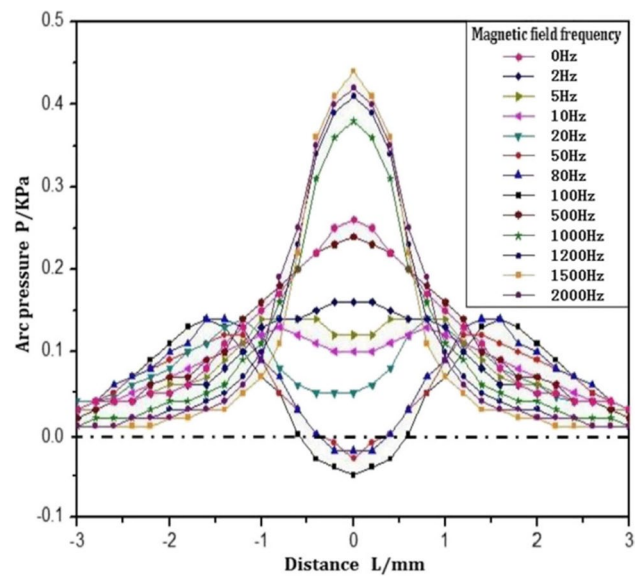


Fig. 12 The distribution of arc pressure [58]

microstructure using electromagnetic oscillation is more refined, and the weld joint strength is higher.

2.4 LBW

Since the birth of laser welding, it has attracted much attention. In the twenty-first century, LAW has become one of the most promising welding technologies. Compared with arc welding, LBW has high energy density, fast welding speed, and small welding deformation. Due to the narrow FZ and HAZ of LAW, it is very attractive for FSS welding [60–62]. At present, scholars have carried out a lot of research on the LAW of FSS. Lakshminarayanan et al. [63] found that when the welding speed is 3000 mm/min, a single-pass full penetration weld without defects can be obtained. The microstructure of the weld joint at different positions and BM is shown in Fig. 14. From Fig. 14 (b) and Fig. 14 (e), it can be found that the FZ is composed of dendrites and equiaxed crystals. The problems of coarse grains and large brittleness that often occur in arc welding of FSS do not appear in LAW. Due to the relatively low heat input of laser welding, the grain size of LBW weld high-temperature heat-affected zone (HTHAZ) is very similar to that of BM with low-carbon grain boundary martensite. Compared with the BM, the impact toughness of LAW is improved by 3%, which is caused by equiaxed crystals and columnar dendrites perpendicular to the crack path.

Liu et al. [64] used LAW to weld 26Cr-3.5Mo FSS. The study found a narrow equiaxed crystal zone in the weld center when the welding heat input is low. The study found that at first, there was a small equiaxed crystal zone in the center of the weld. When the welding heat input increases,

Fig. 13 Trajectories of charged particles in a TIG arc [58]

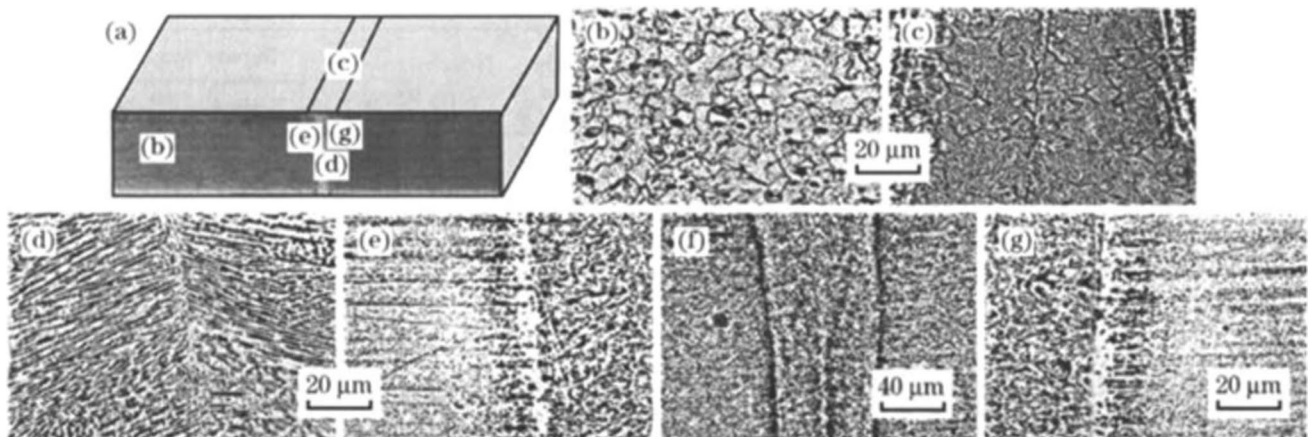
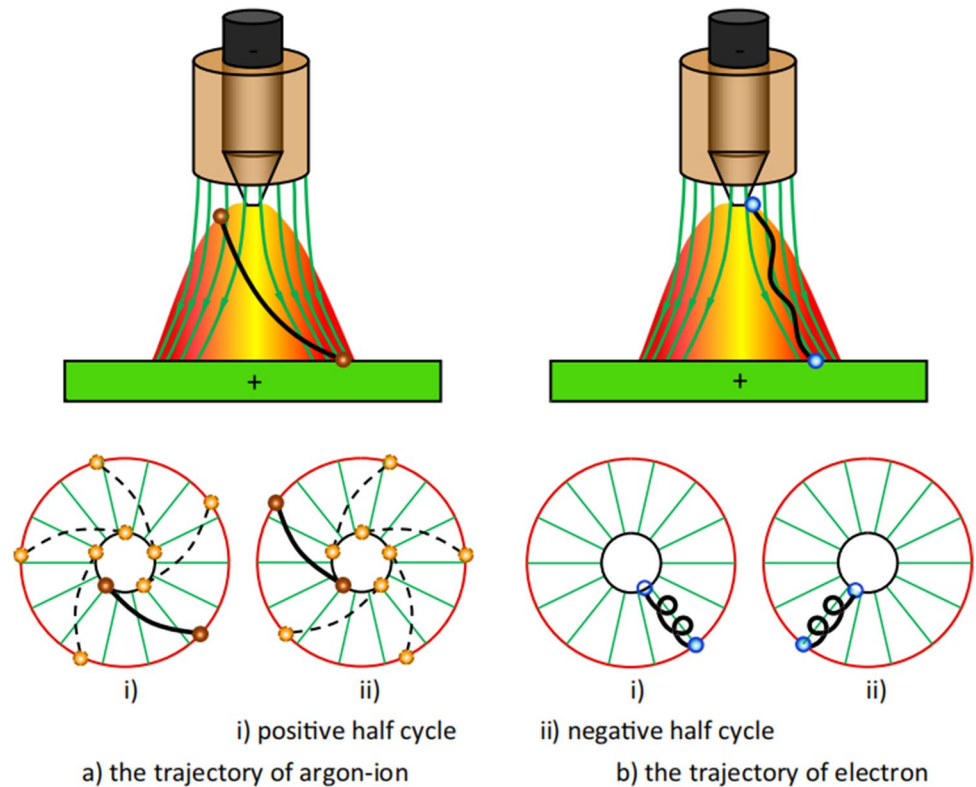


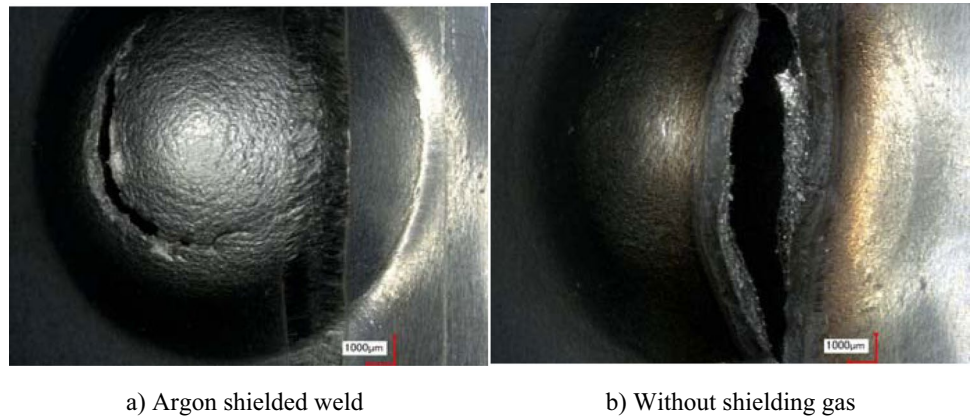
Fig. 14 Optical micrographs of laser beam welded 409 M ferritic stainless steel joint [63]. (a) Joint; (b) base metal; (c) fusion zone top region; (d) fusion zone cross section middle; (e) interface left sides (f) joint cross section; (g) interface right side

the width of the equiaxed crystal zone becomes larger, but the proportion of the cross-section of the weld increases first and then decreases. The microhardness is lower than that of the weld and the BM. The tensile strength of the welded joint is lower than that of the BM, and the elongation of the joint gradually decreases with the increase of heat input, and the fracture mode changes from ductile fracture to brittle fracture. Keskitalo et al. [65] used Erichsen cutting tests to study the influence of shielding gas on the mechanical

properties of FSS LAW. As shown in Fig. 15, the toughness and formability of welds without argon protection are poor. Regardless of the welding energy, the toughness and formability of the weld with argon protection are very good. This is due to the presence of oxide inclusions in the weld metal without gas shielding.

Although LAW has a high energy density and a fast cooling rate, it can solve the grain coarsening of FSS to a certain extent. However, the laser beam utilization rate

Fig. 15 The Erichsen cupping test samples for laser weld samples $E = 90 \text{ J/mm}$, welded with and without argon shielding [65]. a) Argon shielded weld. b) Without shielding gas

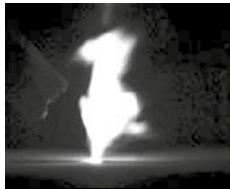
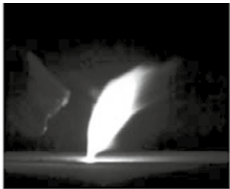
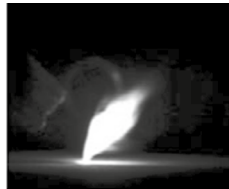
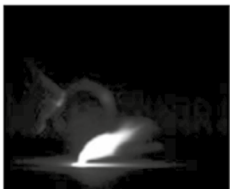




is low, and the cost will increase with the increase of the thickness of the workpiece, and other problems need to be solved urgently. Ma et al. [66] studied the application of a variety of commonly used activating flux in LAW of FSS. The experimental results show that oxide has the most significant effect on the penetration, and the penetration can be increased by 2.23 times within a suitable ratio range. Table 1 shows the high-speed photographs of welding with different activating flux when the laser power is 1600 W. As shown in the figure, except for activating flux CaF_2 , the size of other plasma is proportional to the penetration depth. The

metal added with the oxide activating flux produced violent evaporation. After adding CaF_2 , the size of the plasma is smaller, and the penetration depth is larger. This is because CaF_2 evaporation reduces plasma volume and increases the metal's absorption rate of the laser beam. This also shows that reducing the plasma volume has little effect on increasing the penetration depth of LAW.

The pressure vessel is usually a cylindrical shell with a diameter of about 3.3 to 4.6 m, a height of 12 to 14 m, and a wall thickness of about 230 mm. It is usually welded by Submerged Arc Welding (SAW). However, SAW has some

Table 1 High-speed photographs with different activating fluxes at 1600 W [66]

Activating flux	ZrO ₂	CaO	MgO
High-speed photograph			
Penetration depth / mm	1.60	1.40	0.82
Activating flux	CaCO ₃	CaF ₂	Without flux
High-speed photograph			
Penetration depth / mm	0.60	0.68	0.53

disadvantages, such as large heat input and large residual stress after welding. The narrow gap multi-channel fiber laser welding process provides a new method for welding thick plate FSS. Compared with arc welding, the number of welding passes of narrow gap multi-channel fiber laser welding is greatly reduced [67], which increases the welding efficiency. Figure 16 is a Schematic representation of narrow gap multi-pass laser welding process with filler wire addition. In the welding process, the defects such as cracks, non-fusion, and pores can be eliminated by reasonable control of experimental parameters such as shielding gas. The test has completed the high-quality welding of thick plates, but it is recommended to perform PWHT to improve toughness [68].

2.5 PAW

PAW is a compression arc welding method. It has the advantages of fast cooling, fast welding speed, narrow weld zone, large penetration, high mechanical strength, small deformation, and no need for filler metal during welding [69, 70]. Because PAW has more concentrated arc energy density and higher arc stiffness than GTAW. Therefore, the heat provided per unit length is smaller, and the weld can get finer grains and higher impact toughness, which is more suitable for FSS welding [71].

KÖSE et al. [72] studied the effect of different heat inputs on the PAW welding of FSS. Studies have shown that with the increase of heat input, the tensile strength and hardness of welded joints are reduced. After PWHT, the tensile strength of the welded joint is reduced. The reason for This result is that the weld microstructure softened and transformed after being kept at 7700 °C for 60 min. Hariharan

et al. [73] studied the influence of the PAW process on the corrosion resistance and strength of AISI 409 FSS joints. The response surface method is used to obtain the best combination of welding parameters, the strength of the welded joint is maximized, and the corrosion rate is minimized. As shown in Fig. 17, the corrosion rate of the welded joint is very high. When the optimized welding parameters are used, the resistance increases, the corrosion rate decreases, and the corrosion resistance is improved.

Zhu et al. [74] used a perforated-plasma-arc-welded welding process to weld 00Cr11NbTi FSS. Preformed-plasma-arc-welded is suitable for welding stainless steel plates with a thickness of 3~8 mm and can complete single-pass full penetration welding with square groove. The experimental results show that under the premise of good assembly, the weld is easy to obtain a smooth surface. The bending experiment in Fig. 18 shows that the weld after perforated plasma arc welding, whether on the surface or the back, whether in the horizontal or vertical direction, has good plasticity.

Micro-plasma welding is a kind of low current (usually less than 30A) penetration welding process. It has the characteristics of good arc stiffness, good stability, and excellent welding quality. It is especially suitable for welding FSS sheets. To ensure the stability of the arc at low current, the micro-plasma welding uses a small aperture compression nozzle and combined arc. There are two arcs in welding one is the non-transferred arc between nozzle and electrode, which plays the role of arc striking and arc stabilizing. The other is the transferred arc between the electrode and the workpiece, which is used to melt the workpiece. Low current and low heat input can inhibit the high-temperature embrittlement of FSS to a certain extent [75].

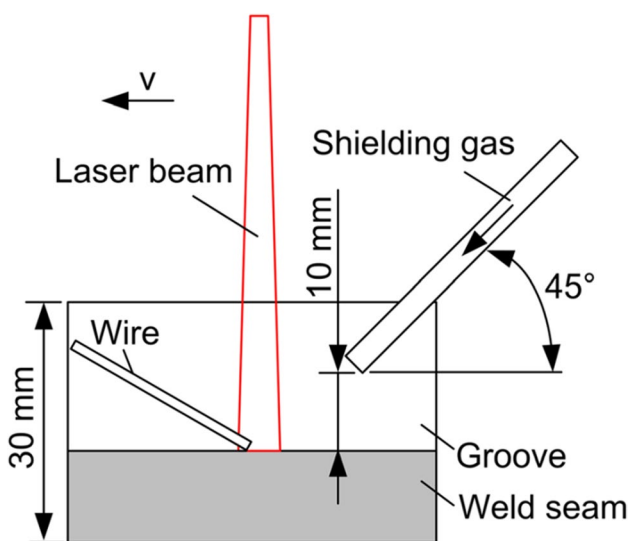


Fig. 16 Schematic representation of narrow gap multi-pass laser welding process with filler wire addition [68]

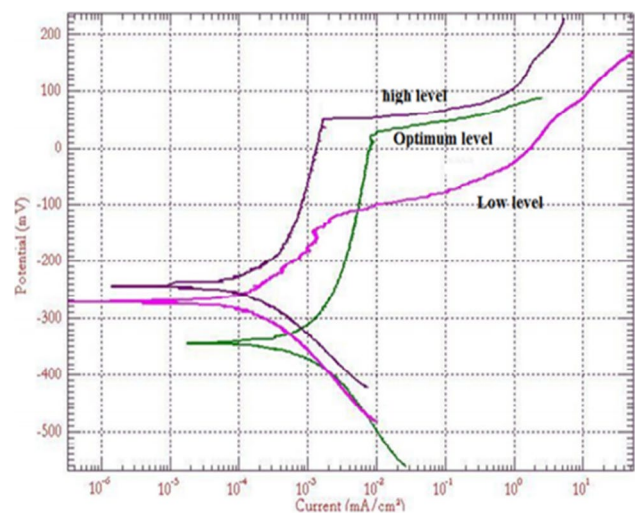
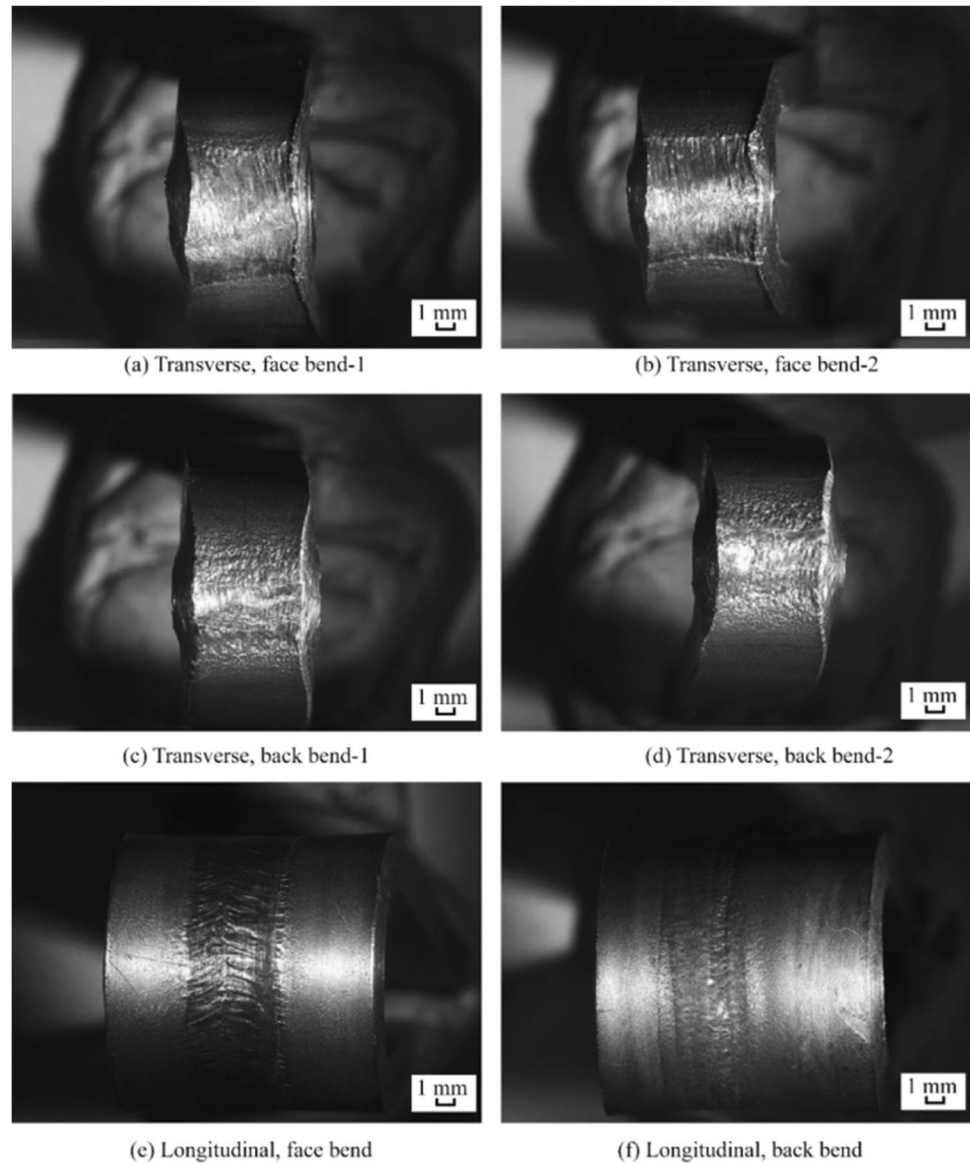


Fig. 17 The Polarization curve for PAW joints [73]

Fig. 18 Bending test results [74]



2.6 EBW

EBW is a welding method that uses a high-energy electron beam as a heat source for welding in a vacuum environment. Since welding is performed in a vacuum environment, material contamination is avoided. EBW has a smaller FZ and HAZ and a larger depth to width ratio. It can produce deep and narrow welds without defects [76], which is attractive for welding FSS.

Lakshminarayanan et al. [77, 78] studied the joint microstructure and properties of AISI409M FSS EBW and compared them with GTAW joints. The experimental results show that the impact toughness of EBW welded 12% Cr FSS joint is similar to that of BM, but the impact toughness of GTAW joint is worse than that of BM, which depends on the microstructure. When GTAW is welding FSS, the

temperature of FZ and HAZ will reach over 1300 °C. During the cooling process, the structure will transform from δ ferrite transforms to austenite. The relative amount of stable elements of ferrite and austenite determines a certain amount of austenite at the grain boundary. The grain size of GTAW weld is large, and the cooling rate is not enough to cover the ferrite grain boundary, so acicular martensite is formed. Coarse grains and acicular martensite are the reasons for the poor toughness of GTAW welds. Due to the low heat input of EBW, fast cooling rate of weld, limited grain growth, and hindered transformation from δ ferrite to austenite, the formed microstructure is composed of ferrite and there is a discontinuous martensite network along the grain boundary, as shown in Fig. 19(d). Therefore, EBW joints have higher fatigue strength and fatigue crack resistance than GTAW joints and BM [79, 80].

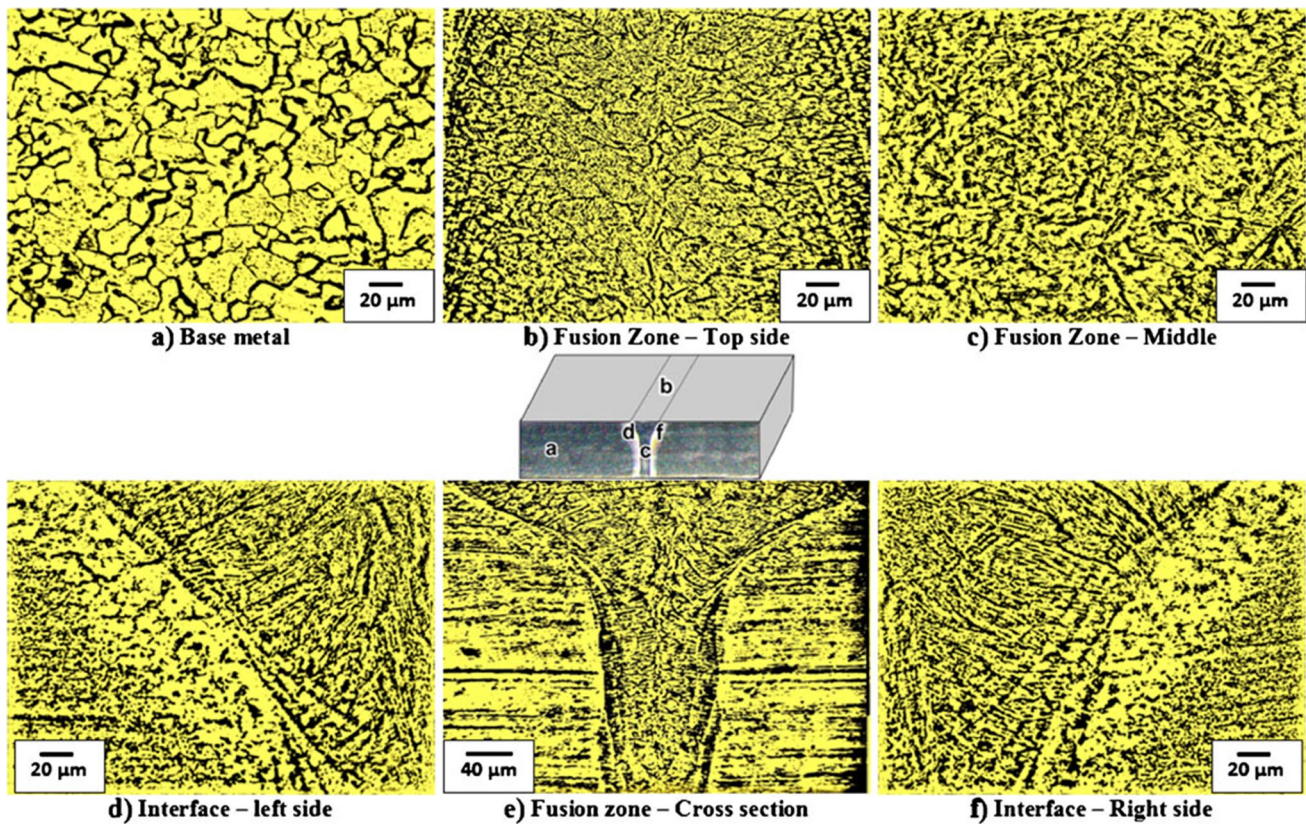


Fig. 19 Microstructure of electron beam welded 409 M ferritic stainless steel joint [77]

Doomra et al. [81] used EBW to complete the deep penetration welding of 18 mm thick AISI409 FSS. The study found that the weld microstructure is composed of coarse columnar crystals growing perpendicular to weld center. The tensile strength, yield strength and microhardness of the WZ are higher than those of the BM, but the impact toughness decreases by 45%. After PWHT, the grain size of the weld is refined, and the impact toughness increases by 40%. Therefore, PWHT is beneficial to improve the toughness of welded joints.

2.7 FSW

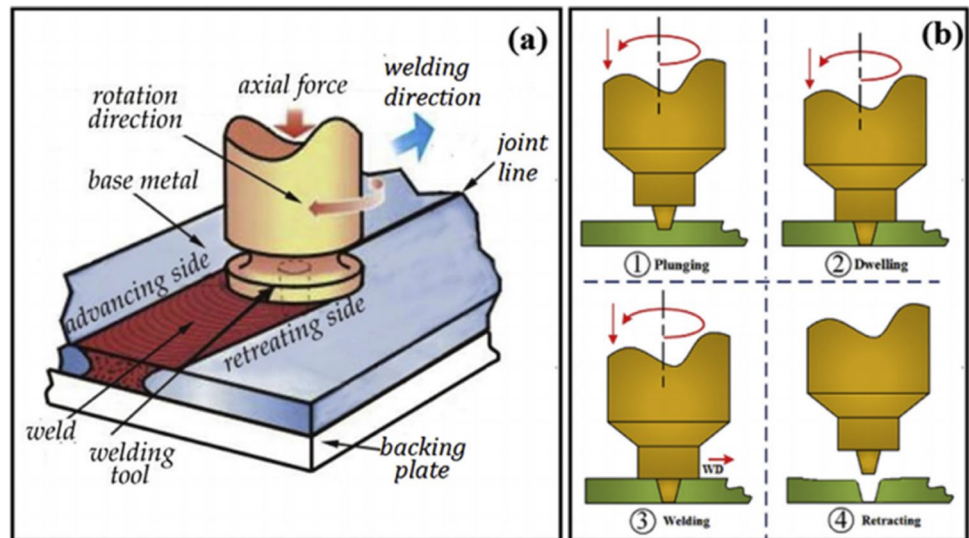
Figure 20 shows a typical FSW welding process. During welding, the welding stirring head rotates at high speed in the direction of the welding seam to increase the temperature of the workpiece. After the temperature rises, the joints of the workpieces are softened. Finally, pressure is applied to promote the diffusion and mutual dissolution of the metal at both ends of the weld to complete the welding. Compared with fusion welding, FSW avoids adverse metallurgical reactions. During welding, dynamic recrystallization occurs in the weld seam, the grains are refined, and the HAZ grains

do not grow significantly [82–84]. Therefore, scholars have done a lot of research on FSW welding FSS.

Lakshminarayanan et al. [85, 86] used FSW to conduct welding tests on 409 M FSS. The welding speed is 50 mm/min, and the rotation speed is 1000 rpm. After welding, it is found that the BM has severe plastic deformation due to friction stirring. This results in the transformation of the coarse ferrite structure in the matrix material to the fine ferrite and martensite dual-phase microstructure. Afterward, the process optimization of 409 M FSS FSW was carried out, and it was found that the welding speed was the main factor affecting the tensile strength and impact toughness. Salemi et al. [87] used FSW to weld AISI430 FSS. The experimental results found that under constant speed conditions, increasing the rotating speed and heat input can achieve dynamic recrystallization of the weld, thereby achieving grain refinement.

Ahmed et al. [88] used FSW to weld AISI 409 ferritic stainless steel and studied the effects of rotation speed and traverse speed on the evolution of weld microstructure. Research has found that high rotation speed will cause a large amount of strain in the metal and reduce the crystal grains.

Fig. 20 FSW process (a) schematic, and (b) various stages [82]



Sharma et al. [89] studied the microstructure and properties of 409 FSS FSW welds. A defect-free welded joint was obtained. The study found that there are martensite and Cr_{23}C_6 precipitates that have the effect of grain refinement at the grain boundaries of the stirring zone. The tensile strength of the welded joint is close to that of the BM, but the ductility is reduced. Due to precipitates Cr_{23}C_6 in the stirring zone, the corrosion resistance is not as good as the HAZ and BM.

Mondal et al. [90] used the element mapping method to conduct a detailed study on the material flow in the ASS and FSS stirring zone. As shown in Fig. 21, the EPMA Electron Probe Micro Analyzer (EPMA) mapping clearly shows that the FSW process depends on the combination of process parameters. The heat generated by parameter 1500/50 is higher, the deformation is more serious, and the grains in the stirring zone increase additionally.

Bilgin et al. [91] studied the influence of FSW rotation speed, traverse speed, tool compression force, and tool inclination angle on the strength of welded joints. Through the establishment of a genetic algorithm model, the best parameters are found, the ultra-fine grain weld microstructure is obtained, and the high-quality welded joint is formed.

Induction preheating friction stir welding is a welding method in which electromagnetic induction coils are added for preheating in FSW. Because FSS is magnetic, electromagnetic induction preheating has a more obvious effect on FSS. As shown in Fig. 22, the induction device is made of copper tube coils. The essential parameters of induction heating setup are the output current, which is responsible for the quantity of heat input, and the frequency which controls the depth of heating. Because preheating reduces tool wear in the welding process, reduces the tool debris in the weld, so the impact toughness is improved [92].

2.8 RSW

RSW is one of the most mature welding methods in industry, and it can weld almost all metals. RSW is a method of welding by heating and pressing at the same time [93, 94]. RSW has high production efficiency, low heat input, does not require filler metal during welding, is not easy to produce secondary phase changes, and is easy to reduce the grain size. It has a certain prospect for welding FSS [95].

Alizadeh-Sh et al. [95] studied the microstructure and properties of AISI430 FSS RSW welds. As shown in Fig. 23, the microstructure of the FZ is dominated by columnar ferrite. There are carbides and martensite phases in the grain boundaries. There is no formation of high-temperature austenite in the high-temperature heat-affected zone (HTHAZ), so the ferrite grains grow up sharply. Due to the fast heat dissipation rate, the transformation of ferrite to austenite at high temperatures is inhibited, so no martensite phase is formed at the grain boundary in this region. The transition from ferrite to austenite occurs in the medium temperature heat-affected zone (MTHAZ). The martensite microstructure is formed after cooling, so it is composed of ferrite and martensite. The formation of austenite at high temperature is an important factor hindering the growth grains. The low-temperature heat-affected zone is characterized by the precipitation of fine chromium carbides in the ferrite grains. Coarse grains are the main factor leading to the decrease of mechanical properties, but as the welding current increases, failure occurs at the position of the BM. The reason is that under higher heat input, due to the increase of the FZ size, the peak load and energy absorption of the weld are increased. There are similar reports in the literature [96]. The welding current of RSW affects Tensile Shear Strength, Nugget Size, and Failure Energy, but has little effect on the microhardness of the FZ. The reason is that the change of

Fig. 21 Material flow diagram with process parameter combination of 1000/50 and 1500/50: material flow behavior diagram (a), and material flow diagram (b) [90]

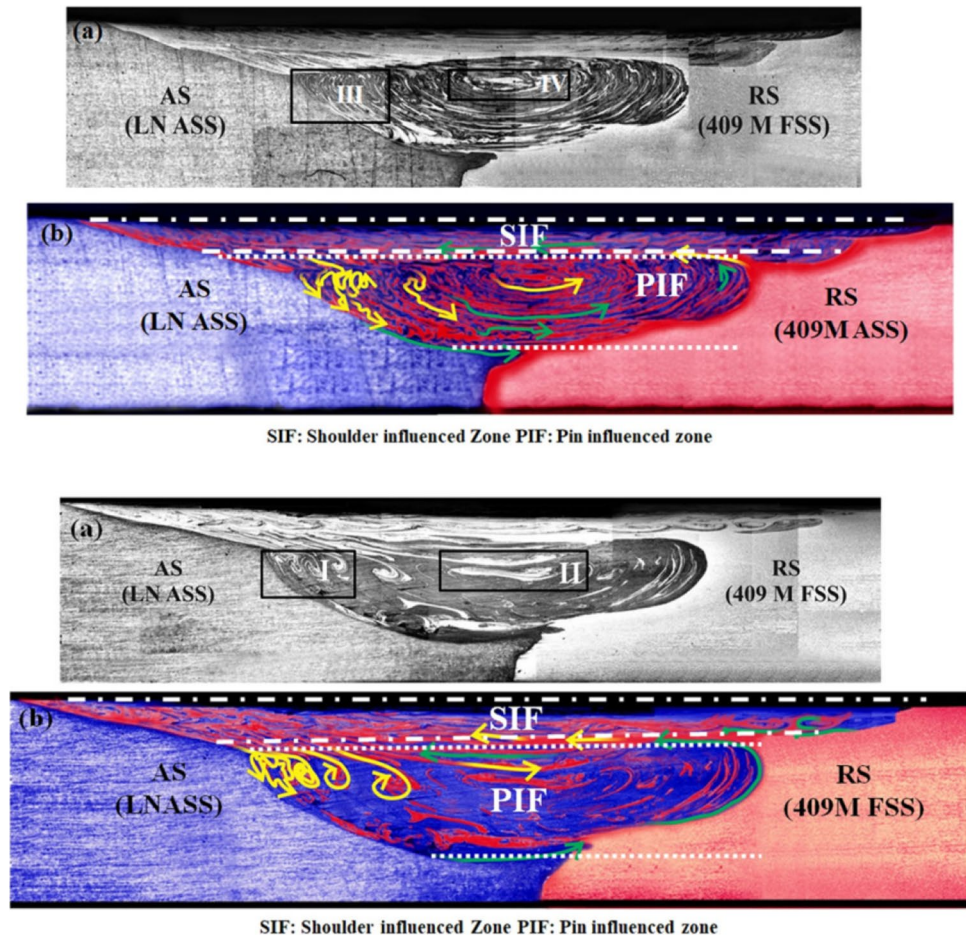
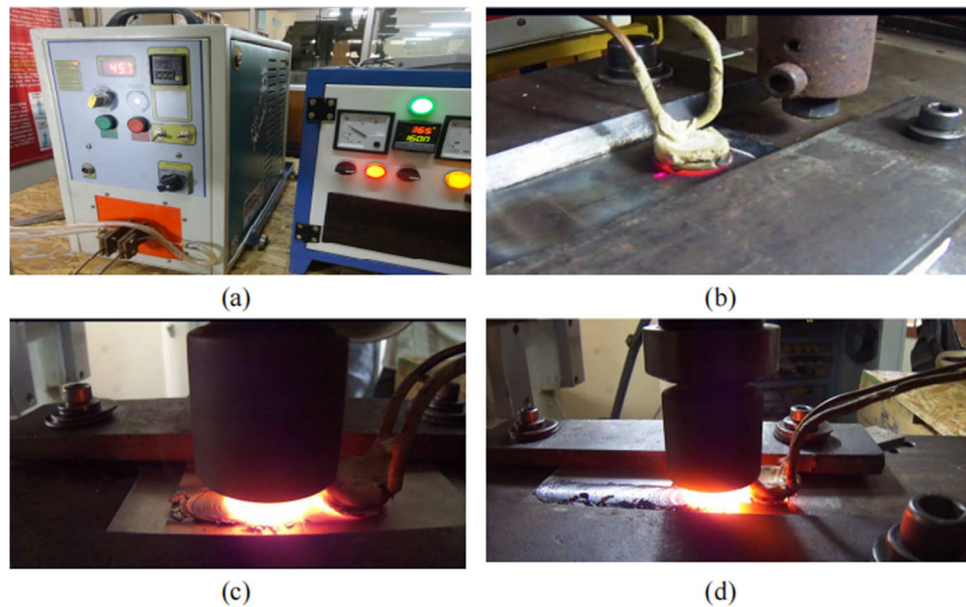


Fig. 22 Electromagnetic induction heating setup and FSW trials [92]



current has an effect on the geometric characteristics of the nugget (such as the diameter and penetration of the nugget) but has no effect on the metallographic aspects (such as the

microstructure and grain size). Existing studies have proved that the microstructure under different currents comprises of ferrite and martensite [96].

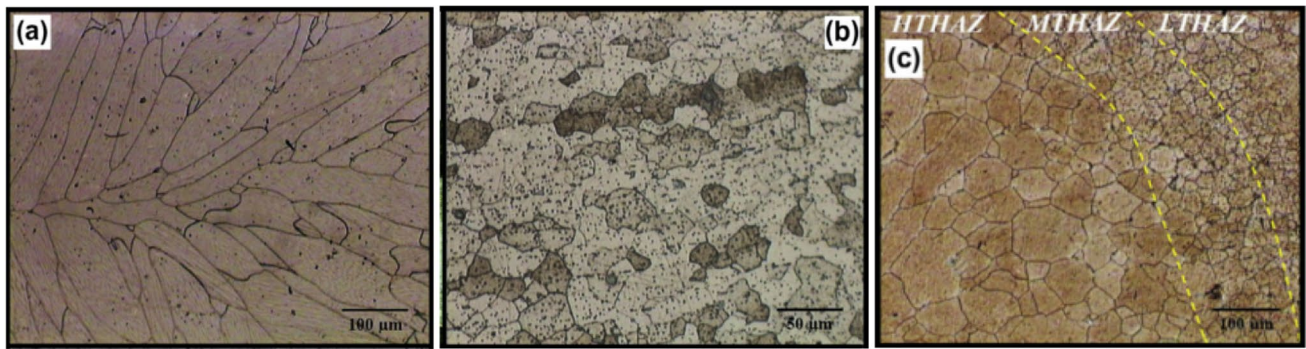


Fig. 23 (a) Fusion zone microstructure, (b) base metal microstructure, (c) heat-affected zone microstructure [95]

The use of austenitic-ferritic composite stainless steel structure is a very promising method that can minimize nickel consumption. Yu et al. [97] compared the mechanical properties of 304/304, 304/430, and 430/430 resistance spot welded joints. The study found that for the 430/430 sample, the nugget is very brittle. The local toughness of the 304/430 weld nugget is higher than that of the 430/430 weld nugget. 304/430 joint has better fracture resistance when the nugget is a brittle fracture. In addition, scholars have conducted a lot of research on the influence of welding parameters such as welding time, extrusion time, shielding gas, and welding current on the strength, toughness, and appearance of RSW.

Ravichandran et al. [98] studied the influence of welding time, extrusion time, welding current, and holding time on the strength of AISI430 FSS by response surface method. The optimal control parameters for higher welded joint strength are obtained. Sreehari et al. [99] studied the effects of welding time and shielding gas on various properties of FSS welded joints. The experimental results show a positive linear relationship between surface indentation and welding time, and the tensile shear strength and nugget diameter increase with the increase of welding time. The purge of argon gas does not affect on tensile strength, indentation degree, hardness, and microstructure, but it helps to suppress heat is tonal.

In addition to the above welding parameters, the electrode material also has an important influence on the results of RSW. CuCo_2Beh and CuZr are both electrode materials for RSW. During welding, the weld joint strength of the two electrodes increases with the increase of current, but the welding parameters of the peak load are different. When the welding current is 6kA, the welding time of the CuZr electrode is 10 cycles, and when the welding current of the CuCo_2Beh electrode is 6.6kA, the welding time is 15 cycles. This is because the conductivity of the electrodes is different. The conductivity of the CuZr electrode is about twice that of the CuCo_2Beh electrode [100].

To solve the bad influence of the organizational transformation, the double Pulse Resistance Spot Welding

technology was proposed [101]. As shown in Fig. 24, a secondary current pulse is induced after the first welding current pulse to achieve the effect of PWHT. Experiments show that the hardness value of the double-pulse welded joint is higher than that of the single-pulse welded joint, and a welded joint with good tensile strength and indentation value is obtained.

Electromagnetic pulse spot welding can be used to weld materials such as Al and stainless steel. The introduction of an external magnetic field can improve the microstructure and properties of RSW [102, 103]. Ding et al. [104] welded FSS with an external static magnetic field spot welding process and found that the diameter of the nugget increased with the increase of welding time. The introduction of a magnetic field can prolong the solidification period of the nugget and hinder the rapid formation of columnar crystals.

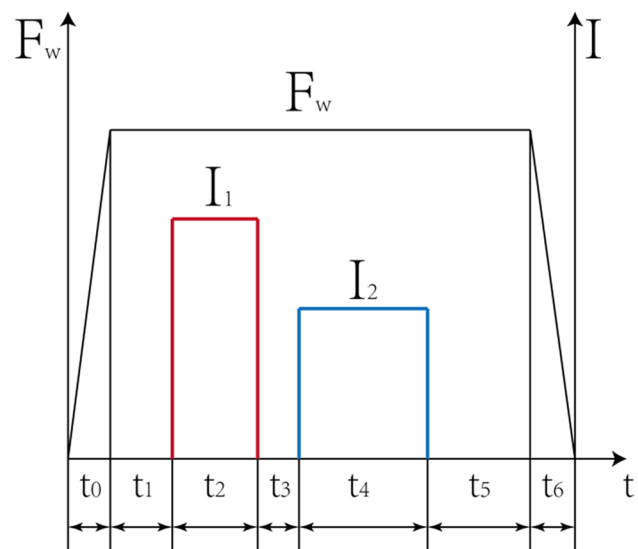


Fig. 24 Double Pulse Technology, t_0 -upslope force time, t_1 -squeeze time, t_2 -time for first pulse current, t_3 -time between two pulses of current, t_4 -time for second pulse, t_5 -hold time, t_6 -downslope force time [101]

The electromagnetic force generated by the magnetic field causes the columnar dendrites to deform, break, and deviate from the solidification direction. As the welding time increases, the grains are refined. However, as the magnetic field increases, the induced current will increase, resulting in a large amount of Joule heating, reducing undercooling, and coarsening of crystal grains. Therefore, proper application of static magnetic field can improve the tensile strength and elongation of spot welded joints.

2.9 Hybrid welding

Hybrid welding is an efficient welding method. It has the advantages of improving the energy utilization rate of the heat source, increasing the welding speed, increasing the penetration depth, and improving the welding quality. It is the trend of future development [39]. In recent years, scholars have tried to use different hybrid welding methods to study the welding of FSS.

Wu et al. [105] used laser-GMAW hybrid welding to weld FSS. Laser-GMAW hybrid welding makes up for the shortcomings of GMAW's slow welding speed, shallow weld penetration, and large heat-affected zone width. At the same time, it also makes up for the disadvantages of high assembly requirements of LAW parts and low gap bridging ability [106, 107]. The research adopts the numerical simulation method to quantitatively analyze the shape and size of the molten pool and small holes, as well as the temperature field and flow field in the mixed molten pool. As shown in Fig. 25, the small hole in the front of the molten pool blocks the flow circuit driven by the surface tension gradient at the front of the molten pool. At the same time, the periodic impact of the molten droplet and the instantaneous collapse of the small hole cause the molten pool to fluctuate, blocking the loop driven by the surface tension gradient at the tail of the molten pool. Therefore, there is a small amount of eddy current on the surface of the molten pool, which has a stirring effect on the molten pool and helps the welding of FSS.

Laser + Pulsed Gas Metal Arc Welding (Laser + GMAW + P) has high welding speed, low heat input, narrow HAZ, large penetration, strong bridging ability, and stable welding. For the use of Laser + GMAW + P to weld FSS, it is necessary to understand the influence of mixed heat sources on the HAZ and its grain growth behavior. Zhang [108] et al. simulated the grain microstructure of the HAZ of FSS under the hybrid heat source of Laser + GMAW + P. Figure 26 is the final three-dimensional map of the grain microstructure of the HAZ. As shown in the figure, the closer the fusion line, the finer the grains, but the grain size is different at different positions on the fusion line. The grain size below the molten pool is much smaller than the top of the molten pool, and the grain sizes are similar to LAW. This is because the penetration of hybrid welding

is determined by the laser beam, the heating and cooling time is very fast, the growth time of grain is short, and the grain size is limited. It is verified by experiments that there are certain errors in the shape and size of the HAZ, and the simulation and measurement should be improved.

Zhang et al. [109] designed the plasma + TIG hybrid welding method. PAW is used as the backing welding method, and the TIG welding method is used for cosmetic welding. The research results show that proper acceleration of the welding seam cooling rate is helpful to the refinement of the weld seam structure. The plasma flow rate has little effect on the grain size.

Hybrid Friction Stir Welding (HFSW) is a hybrid welding process that uses GTAW as the preheat source for FSW. Figure 27 is a schematic illustration of HFSW process and FSW tool without pin. GTAW as a preheat source can slow down the cooling rate after welding, improve material flow, and improve mechanical properties. At the same time, similar to induction preheating friction stir welding [92], the preheating source has the effect of reducing tool wear. The results show that the welded joint of HFSW has better ultimate tensile strength and elongation than that ordinary FSW [110].

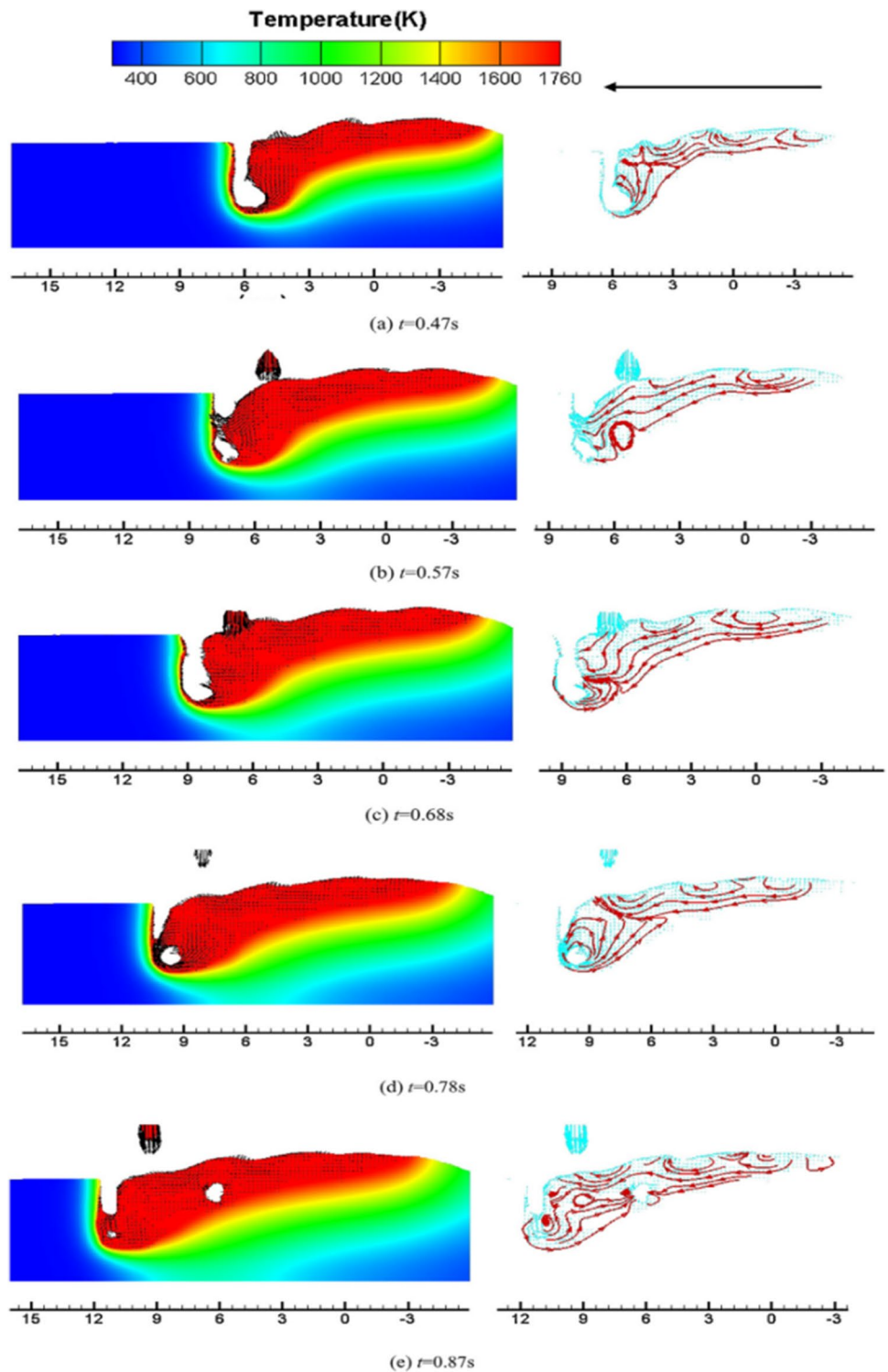
3 Trend of development

In summary, in the welding method of FSS, we can summarize some rules from the traditional and improved welding methods and then control the future development direction of FSS welding (Table 2).

It can be seen from the Table 2:

- (1) When using SMAW welding, the welding equipment is simple, the operation is flexible, and the welding efficiency is high. However, welding heat input is large, resulting in the coarse grains in the welding HAZ and the serious loss of the plastic toughness of the welded joint. To improve the performance, the impurity content in the electrode should be limited as far as possible, its purity should be improved, and reasonable alloying should be carried out at the same time. However, when welding thick plates, grooves are required, which seriously reduces the welding efficiency. Therefore, it is not recommended.
- (2) When using GMAW welding, the welding efficiency is high. Usually, the austenite welding wire is used for welding. By introducing austenitizing elements, more austenite is formed to hinder the growth of ferrite grains in the weld. In addition, by adjusting the chemical composition of the filler materials of GMAW and FCAW, the weld microstructure can be refined, and the plastic toughness of the welded joint can be improved. However, due to excessive welding heat input, the width

Fig. 25 The dynamic evolution of temperature profile and fluid flow field in longitudinal cross-section of weld pool [105]



and grain size of the HAZ of the joint will increase. When using P-GMAW and DP-GMAW welding processes, by applying current pulses, the total welding heat input can be accurately controlled, and the growth of the HAZ grains can be restricted. In addition, the pulse current will generate a pulsating magnetic field

in the molten pool. According to the electromagnetic field theory, the liquid metal particles in the molten pool are subjected to the pulsating electromagnetic force to produce vortex motion, which causes the force gradient change. The difference in contraction force at different positions causes the flow velocity of the

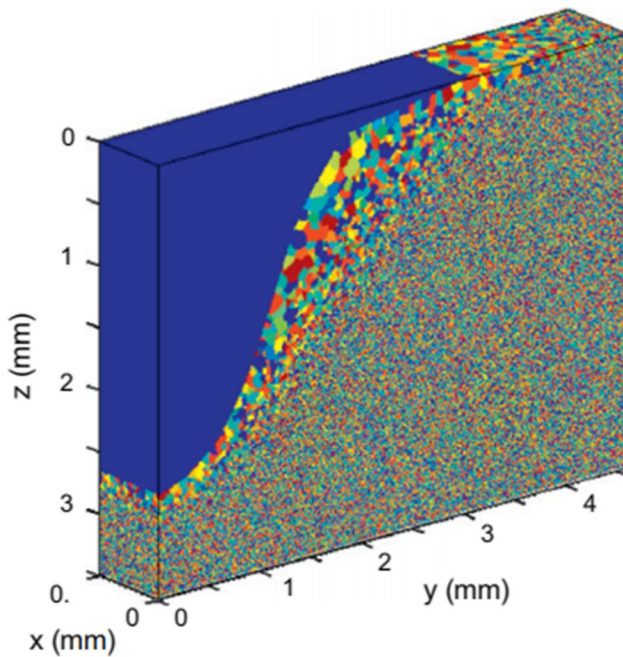


Fig. 26 3D map of the grain structure of the HAZ [108]

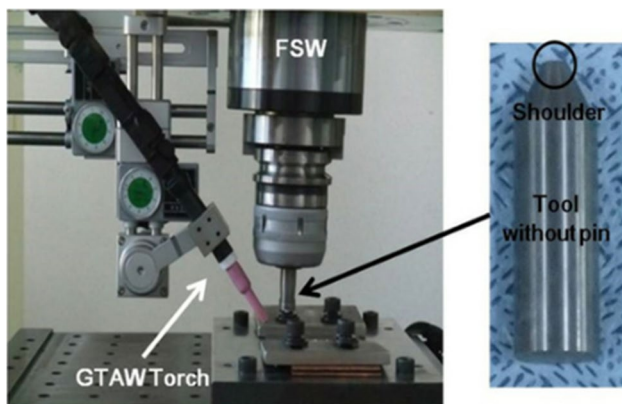


Fig. 27 Schematic illustration of HFSW process and FSW tool without pin [110]

molten pool metal to change, creating a velocity gradient. According to Newton's law of viscosity, the velocity gradient will cause shear force in the molten pool, and the shear force will break up the columnar crystals produced during the solidification of the liquid metal in the molten pool, and finally form fine equiaxed crystals. In addition, from the perspective of metal crystallization thermodynamics, the complex flow in the molten pool promotes the uniformity of the liquid metal in the molten pool, reduces the liquid phase temperature gradient, promote the transformation of coarse dendrites to fine equiaxed crystals.

- (3) At present, GTAW is one of the most suitable welding methods for welding FSS. Compared with SMAW and GMAW, GTAW has smaller heat input, smaller grain size in the welding HAZ, and no consumables during autogenous welding. However, due to its low welding efficiency and scattered arcs, resulting in shallow weld penetration, it is only suitable for welding steel plates of 2 mm or less. When welding thick plates, M-TIG can be used, but multi-layer and multi-pass welding will reduce welding efficiency and increase consumables. A-TIG and K-TIG are derived based on TIG welding. The purpose is to compress the welding arc, make the arc energy density more concentrated to obtain greater penetration depth, complete the one-time autogenous welding of thick plates, and improve welding efficiency. However, the surface of the A-TIG weld is poorly formed. The microstructure of the K-TIG WZ is symmetrically grown coarse columnar crystals, so the weld has poor toughness. P-GTAW is easy to control the welding heat input. The solidification process of the liquid metal in the weld is similar to that of the P-GMAW process, and it is easy to obtain a refined weld microstructure. When using U-TIG welding, ultrasound has the effect of refining the weld grain. First of all, ultrasound has a mass transfer effect. The finite-amplitude attenuation of the ultrasonic wave in the liquid metal of the welding pool causes a certain sound pressure gradient in the melt. The sound pressure gradient can cause the liquid metal to spray, causing the liquid metal to create circulation, resulting in the crystallization of the unfinished columnar crystal is broken, thus achieving grain refinement. Secondly, ultrasound has a cavitation effect in liquid metal; that is, the tiny bubbles collected in the liquid are activated under the action of ultrasound, which manifests as a series of nonlinear dynamic processes such as the vibration, growth, contraction, and collapse of the bubble core [112]. Cavitation will impact the liquid metal in the molten pool, which can break up coarse columnar crystals, increase new nucleation particles, and increase the nucleation rate. In addition, ultrasonic waves also have the effect of acoustic streaming. When strong sound waves propagate in the medium, a non-periodic flow will often appear. This phenomenon is called acoustic streaming. During the welding process, the liquid metal in the molten pool will produce convection under the acoustic streaming, which will break up the growing coarse dendrites, increase new nucleation particles, and increase the nucleation rate. Under the action of the above three mechanisms, the molten pool metal will flow vigorously, scouring the crystal nuclei at the edge of the molten pool, and crush the growing columnar crystals inside the weld, which will be evenly stirred

Table 2 Welding methods and purposes of FSS

Methods of welding		Improvement method	Purpose of improvement
SMAW		Filled ASS wire	Add alloying elements to improve toughness
GMAW	Traditional MIG	Add chemical elements	Add alloying elements to improve toughness
		P-GMAW	Apply current pulse signal
	DP-GMAW	Apply current double pulse signal	Refine grains, increase toughness, reduce porosity and crack sensitivity
	FCAW	Flux Cored Arc Welding	Refine grains and reduce the sensitized area of the weld
	CMT	Cold Metal Transfer welding	Reduce welding spatter, low heat input, refine grains, improve toughness
GTAW	Traditional TIG	Control heat input	Refine grains, improve toughness
	M-TIG	Multipass tungsten inert gas welding	Suitable for welding thick plates
	A-TIG	Activating flux TIG	Increase penetration and improve corrosion resistance
	K-TIG	Keyhole gas tungsten arc welding	Increase penetration
	P-GTAW	Apply current pulse signal	Control heat input, refine grains and improve weld toughness
		U-TIG	Ultrasonic assisted
		Change the shielding gas	Refine grains, increase the ratio of equiaxed crystals, and improve the strength and toughness
	Add chemical elements	Powder pre-melting technology, Directly add, Coated on the surface of the BM	Refine grains, improve toughness
LBW	Traditional LBW	Magnetic control welding	Compress arc, increase arc energy density and stiffness,
			Increases penetration, increase welding speed, refined grains, and improve strength and toughness
		Control heat input	Increase weld equiaxed crystal, improve toughness
		Change the shielding gas	Increase toughness and control weld formation
	Added activating flux	Increase penetration	
	Narrow gap multichannel fiber laser welding	Welding thick plate, reduce weld bead, increase welding efficiency, eliminate defects	
PAW	Traditional PAW	Control heat input	Refine grains, improve strength, corrosion resistance
	P-PAW	Perforated-plasma- arc-welded	Increase penetration
	Micro-plasma welding	Use a small welding current of less than 30A	Welding thin plate, improve arc energy density and stiffness, increase welding speed, refine grains
EBW	-	-	Increase penetration, avoid weld contamination, improve fatigue strength, and reduce cracks
FSW	Traditional FSW	Control welding speed, rotation speed, tool compression force, and tilt angle	Refine grains, improve strength and toughness
	Induction preheating FSW	Electromagnetic induction coil preheating	Reduce tool wear, reduce tool debris incorporation, improve toughness
RSW	Traditional RSW	Control welding time, extrusion time, welding current, and holding time	Improve the strength
		Change the shielding gas	Suppress the heat is tonal
		Changing electrode material	Improve the strength
	Double pulse RSW	Apply current double pulse signal	Equivalent to PWHT, improve the strength
	Assisted by the external static magnetic field	Refine grains, improve strength and elongation	

Table 2 (continued)

Methods of welding	Improvement method	Purpose of improvement	
Hybrid Welding	Laser-GMAW hybrid welding	Hybrid welding of Laser welding and MIG welding	Increase the welding speed, increase the penetration, reduce the width of the HAZ, reduce cracking and porosity, and refined grains
	Laser + GMAW + P	Laser + Pulsed Gas Metal Arc Welding GMAW	Increase welding speed, reduce heat input, reduce HAZ, increase penetration, increase the bridging ability
	Plasma and TIG hybrid weld	PAW + TIG	Refine grains, improve toughness
	Hybrid Friction Stir Welding	GTAW + FSW	Increase welding speed, improve material flow, reduce tool wear, reduce tool debris mixing, improve toughness

with the molten pool. The dispersion in the molten pool adds new nucleation points, increases the nucleation rate, and promotes the conversion of columnar crystals to equiaxed crystals [112]. But at the same time, ultrasonic vibration also has some shortcomings, such as the ultrasonic welding equipment is not stable enough, an external ultrasonic device is needed, and there is sometimes no continuous ultrasonic modulation, it is difficult to apply in actual production, and the weld is prone to collapse. It adopts magnetic control welding, which has a strong effect on grain refinement. First, according to the principle of electromagnetic induction, when a magnetic field is applied to the molten pool, the liquid metal in the molten pool can be regarded as a current-carrying conductor. Under the action of the applied alternating magnetic field, the electromagnetic force will be generated, and the electromagnetic force will promote the liquid in the molten pool. The metal flows and stirs. The stirring process will break the dendrite growing in the molten pool. The broken dendrite will form many crystal nuclei, which increases the number of crystal nuclei and restricts the growth of crystal grains. In addition, stirring makes the temperature distribution at the front of the solid–liquid interface consistent with obtaining a uniformly refined equiaxed crystal microstructure [113,114]. Secondly, the magnetic field has the effect of compressing the arc and increasing the arc pressure. The segregation of solutes in the liquid metal of the molten pool will cause a “neck” at the intersection of the crystal and the edge of the molten pool. The increase of arc pressure can accelerate the convection of the molten pool and then wash the “neck,” causing the crystal grains to fall off the edge of the molten pool. The separated crystal grains follow the flow of the molten pool and are evenly dispersed in the molten pool. These crystal grains can be used as the original crystal nuclei of new crystal grains in the molten pool. In addition, electromagnetic stirring can reduce the temperature gradient

of the molten pool metal at various positions, reduce the burning loss of metal elements in the molten pool, increase the heterogeneous nucleation of particles, and finally refine the crystal grains.

- (4) Adopt high-energy beam methods such as LBW, PAW, and EBW to weld FSS, which can realize one-time autogenous welding of thick plates. Due to its concentrated energy density and fast welding cooling rate, the width and grain size of the HAZ can be reduced, and the strength and toughness of the joint can be improved. However, LBW is prone to stress and strain concentration during welding, and the weld is easy to sink, and the cracking rate during PAW welding is high. In addition, when the high-energy beam welding method is used, the WZ microstructure is symmetrically grown coarse columnar crystals, and the toughness of the weld is still severely lost compared with the BM, and the price is high.
- (5) When using FSW and RSW, compared to fusion welding, pressure welding avoids unfavorable metallurgical reactions. FSW weld produces dynamic recrystallization, the grains are refined, and HAZ grains do not grow significantly, but it is not suitable for thick plate welding. Tool wear during welding is likely to be incorporated into the weld, reducing the strength and toughness of the weld. The addition of an induction preheating device can reduce the wear of the tool, reduce the incorporation of tool fragments, and further improve the toughness of the welded joint. When using RSW welding, the microstructure and properties of the weld can also be improved by applying current pulses and auxiliary magnetic fields.
- (6) The hybrid welding method has the advantages of improving the welding quality, increasing the welding speed, and increasing the penetration depth. On the one hand, the two welding methods combined can make up for each other's shortcomings. On the other hand, one of the welding methods may also have a preheating effect on the base material and improve the utilization

rate of heat source energy. However, the microstructure of the hybrid welding device is relatively complicated, and the mechanism of action between the heat sources is not yet precise. At present, the relevant research mostly stays in the experiment and numerical simulation stage, and it will take some time to be used in actual production.

With the development of industry and the needs of enterprises, the welding of FSS in the future will develop into thick plates, low consumables, high efficiency, and high quality. Adjusting the welding parameters based on the traditional welding method is not enough to meet such requirements. Among the improved welding methods, scholars have researched deep penetration welding and grain refinement, but the two seem to be contradictory. The reason is that deep penetration welding will inevitably bring about a considerable heat input, resulting in coarse grains in the HAZ. Although some high-energy beam autogenous welding methods can obtain a very narrow HAZ, the weld microstructure is symmetrically grown columnar crystals. These reasons will lead to a severe decline in the toughness of the welded joint. Therefore, improving the joint performance of thick plate high-efficiency autogenous welding has brought new issues to researchers.

In recent years, scholars have conducted a lot of research on welding methods of superimposed external fields, such as superimposed electric fields, magnetic fields, and ultrasonic. One of the documents pointed out [59] that the coupling of high-frequency electric pulses, magnetic pulses, and electromagnetic pulses all have a compressive effect on the arc, which can increase the arc energy density and increase the weld penetration. At the same time, both electric and magnetic pulses have a stirring effect on the liquid metal in the molten pool, which can change the mass and heat transfer processes in the molten pool metal crystallization process, refine the weld microstructure, improve the weld appearance, and reduce weld defects, improve the mechanical properties of the weld. Almost every welding method can enhance the quality of welding under appropriate electric and magnetic field parameters. Therefore, studying the influence of electric and magnetic fields on the welding process of FSS is of great significance to the realization of deep penetration, low consumables, high efficiency, and high quality welding of FSS.

4 Conclusion

FSS has superior performance, low cost, and broad application prospects. However, during welding, especially under high-efficiency welding conditions, the grain size of the WZ and the HAZ grows seriously, resulting in a serious decrease

in the strength and toughness of the welded joint. The existing welding methods have certain limitations. The improved method has an excellent effect on increasing the penetration depth or improving the weld performance. Among these methods, the use of electric and magnetic pulses is more widespread, which can change the motion law of the arc and molten pool, and refine the crystal grains. In addition, high-frequency electric and magnetic pulses will compress the arc and make the arc energy density more concentrated, improve the penetration rate. With the advancement of science and technology, the future of FSS welding will develop towards thick plates, high efficiency, and high quality. Therefore, it is possible to consider applying high-frequency electric and magnetic fields to achieve high-efficiency and high-quality welding of FSS.

Acknowledgements The present research work was financially supported by the Project of the National Natural Science Foundation of China (Grant No.51575362), Major project of Scientific and Technological Achievement transformation of shenyang(Grant No.20-203-5-01), the Ministry of Education and Science of Russian Federation (Grant No.11.9505.2017/8.9).

Author contribution All co-authors participated in the writing or guidance of the paper and played an important role.

Funding The present research work was financially supported by the Project of the National Natural Science Foundation of China (Grant No.51575362). Shenyang ‘Shuangbai’ Project (Grant No. Z17-5-70). Major project of Scientific and Technological Achievement transformation of shenyang(Grant No.20-203-5-01). the Ministry of Education and Science of Russian Federation (Grant No.11.9505.2017/8.9).

Data availability Not applicable. This paper is a review paper.

Declarations

Ethics approval We comply with the COPE guidelines and make the following commitments. The content involved in this manuscript is original. It does not involve publishing in any form or language elsewhere. The quoted words of other people are marked in the text by reference.

Consent to participate All co-authors are aware of the writing and publication of this article and agree to publish it.

Consent for publication All co-authors agree to publish this article.

Competing interests The authors declare no competing interests.

References

1. Mondal M, Das H, Ahn EY, Hong ST, Kim MJ, Han HN, Tapan KP (2017) Characterization of friction stir welded joint of low nickel austenitic stainless steel and modified ferritic stainless steel. *Met Mater Int* 23:948–957. <https://doi.org/10.1007/s12540-017-6845-z>

2. Liu HL, Ma MY, Liu LL, Wei LL, Chen LQ (2019) Effect of W addition on hot deformation and precipitation behaviors of 19Cr2Mo ferritic stainless steel. *J Iron Steel Res Int* 26:425–434. <https://doi.org/10.1007/s42243-019-00233-x>
3. Wu WY, Hu SS, Shen JQ, Ma L, Han J (2015) Sensitization of 21% Cr ferritic stainless steel weld joints fabricated with/without austenitic steel foil as interlayer. *J of Materi Eng and Perform* 24:1505–1515. <https://doi.org/10.1007/s11665-015-1409-1>
4. Okayasu M, Shigeoka T (2019) Effect of microstructural characteristics on mechanical properties of ferritic stainless steel. *J of Materi Eng and Perform* 28:6771–6778. <https://doi.org/10.1007/s11665-019-04426-z>
5. Scalise TC, Oliveira MCLD, Sayeg IJ, Antunes RA (2014) Sensitization behavior of type 409 ferritic stainless steel: confronting DL-EPR test and practice W of ASTM A763. *J of Materi Eng and Perform* 23:2164–2173. <https://doi.org/10.1007/s11665-014-1010-z>
6. Huang XZ, Wang D, Yang YT (2015) Effect of precipitation on intergranular corrosion resistance of 430 ferritic stainless steel. *J Iron Steel Res Int* 22:1062–1068. [https://doi.org/10.1016/S1006-706X\(15\)30113-8](https://doi.org/10.1016/S1006-706X(15)30113-8)
7. Han K, Hong S, Lee C (2012) The effect of the precipitates type on the thermal fatigue properties of 18% cr ferritic stainless steel weld haz. *Mater Sci Eng, A* 546:97–102. <https://doi.org/10.1016/j.msea.2012.03.032>
8. Sello MP, Stumpf WE (2011) Laves phase precipitation and its transformation kinetics in the ferritic stainless steel type aisi 441. *Mater Sci Eng, A* 528(3):1840–1847. <https://doi.org/10.1016/j.msea.2010.09.090>
9. Lakshminarayanan AK, Balasubramanian V (2012) Characteristics of laser beam and friction stir welded aisi 409m ferritic stainless steel joints. *J of Materi Eng and Perform* 21(4):530–539. <https://doi.org/10.1007/s11665-011-9943-y>
10. Lakshminarayanan AK, Balasubramanian V (2012) Evaluation of microstructure and mechanical properties of laser beam welded aisi 409m grade ferritic stainless steel. *J Iron Steel Res Int* 19:75–78. [https://doi.org/10.1016/S1006-706X\(12\)60050-8](https://doi.org/10.1016/S1006-706X(12)60050-8)
11. Silva CC, Farias JP, Miranda HC, Guimarães RF, Menezes JWA, Neto MAM (2008) Microstructural characterization of the HAZ in AISI 444 ferritic stainless steel welds. *Mater Charact* 59(5):528–533. <https://doi.org/10.1016/j.matchar.2007.03.011>
12. Silva CC, Miranda HC, Sant'Ana HBD, Farias JP (2013) Austenitic and ferritic stainless steel dissimilar weld metal evaluation for the applications as-coating in the petroleum processing equipment. *Mater Design* 47:1–8. <https://doi.org/10.1016/j.matdes.2012.11.048>
13. Fu A, Li SS, Zhou K, Fang NW, Li DH (2020) Research on MAG welding technology of T-joint of T4003 ferrite stainless steel. *Welding Digest of Machinery Manufacturing* (01):13–17. CNKI:SUN:HJFC.0.2020-01-004
14. Ruan Q, Li JC, Wang JW (2015) Ferritic stainless steel high temperature heat affected zone microstructure and welding performance analysis. *Foundry technology* 36(6):1554–1558. <https://doi.org/10.16410/j.issn1000-8365.2015.06.064>
15. Wei ZY, Yan ZF, Wang ZN, Xu ZQ, Zhou CL (2016) Infrared fatigue crack proportion of 4003 ferritic stainless steel welded by MIG welding. *Journal of Taiyuan University of Technology* 47(03):289–293. <https://doi.org/10.16355/j.cnki.issn1007-9432t.yut.2016.03.003>
16. Narang R, Maheshwari V, Khanna P (2020) Prediction of bead geometry parameters in MIG welded stainless steel 409L plates by mathematical modelling. *Materials Today: Proceedings* 44(1):900–908. <https://doi.org/10.1016/j.matpr.2020.10.795>
17. Akita M, Uematsu Y, Kakiuchi T, Nakajima M, Agata Y, Takino K (2018) Joint microstructures mechanical properties and fatigue behaviour of ferritic stainless steel sus 430 welds with different filler metals. *Weld Int* 32(6):427–435. <https://doi.org/10.1080/09507116.2017.1346860>
18. Zhang Y, Tan ZX, Xu HJ, Lu X, Tong W (2012) Economical ferritic stainless steel welded head structure and corrosion resistance. *Transactions of the China Welding Institution* 33(12):18–22.
19. Mukherjee M, Dutta A, Kanjila P, Tapan P (2015) Enhancement of microstructural and mechanical properties by pulse mode of metal transfer in welded modified ferritic stainless steel. *ISIJ Int* 55(7):1439–1447. <https://doi.org/10.2355/isijinternational.55.1439>
20. Zhang H, Hu SS, Shen JQ, Ma L, Yin FL (2015) Microstructures and mechanical properties of 30Cr-4Mo ferritic stainless steel joints produced by double-pulsed gas metal arc welding. *Int J Adv Manuf Technol* 80:1975–1983. <https://doi.org/10.1007/s00170-015-7173-4>
21. Venkatesan MV, Murugan N, Sam S, Albert SK (2013) Effect of heat input on macro micro and tensile properties of flux cored arc welded ferritic stainless steel joints. *Trans Indian Inst Met* 67(3):375–383. <https://doi.org/10.1007/s12666-013-0358-3>
22. Kim JM, Lee H (2014) Study for corrosion characteristics of ferritic stainless steel weld metal with respect to added contents of Ti and Nb. *Met Mater Int* 20:329–335. <https://doi.org/10.1007/s12540-014-1019-8>
23. Zhou J, Shen JQ, Hu SS, Zhao GC, Wang Q (2019) Microstructure and mechanical properties of AISI 430 ferritic stainless steel joints fabricated by cold metal transfer welding. *Mater Res Express* 6:11. <https://doi.org/10.1088/2053-1591/ab4770>
24. He SR, Wang WX, Zhang TT, Zhang ZH (2014) Study on HAZ microstructure and properties of ferritic stainless steel CMT welded joint. *Mechanical Engineering & Automation* 05:97–98
25. Delgado-Venegas J, Molina-Díaz A, Ambríz-Rojas RR, Cuenca-Alvarez R (2015) Microstructural, mechanical properties and corrosion resistance of ferritic stainless steel welded by GTAW and coated by flame spraying. *MRS Proc* 1765:1–9. <https://doi.org/10.1557/opl.2015.799>
26. Swati J, Nilesh D, Rajeev A (2015) A study on the effect of welding on HAZ, mechanical properties and corrosion of AISI 409m ferritic stainless steel by SMAW, TIG and MIG welding. *International Journal of New Innovation in Science and Technology* 3(1):1–9
27. Mohandas T, Reddy GM, Naveed M (1999) A comparative evaluation of gas tungsten and shielded metal arc welds of a “ferritic” stainless steel. *J Mater Process Tech* 94(2–3):133–140. [https://doi.org/10.1016/S0924-0136\(99\)00092-8](https://doi.org/10.1016/S0924-0136(99)00092-8)
28. Ranjbarnodeh E, Hanke S, Weiss S et al (2012) Effect of welding parameters on the heat-affected zone of AISI409 ferritic stainless steel. *Int J Min Met Mater* 19:923–929. <https://doi.org/10.1007/s12613-012-0648-5>
29. Mousazade MA, Haghighi RD (2020) Autogenous tungsten inert gas welding of 430 Ferritic stainless steel the effect of inter-pass temperature on microstructure evolution and mechanical properties. *J Mater Eng Perform* 29:7807–7820. <https://doi.org/10.1007/s11665-020-05281-z>
30. Amuda H, Mridha S (2011) Effect of energy input on microstructure and hardness of tig welded aisi 430-ferritic stainless steel. *Advanced Materials Research* 264–265:390–396. <https://doi.org/10.4028/www.scientific.net/AMR.264-265.390>
31. Wang YC, Ding M, Zheng Y, Liu SS (2016) Finite-element thermal analysis and grain growth behavior of HAZ on argon tungsten-arc welding of 443 stainless steel. *Metals-Open Access Metallurgy Journal* 6(4):77. <https://doi.org/10.3390/met6040077>
32. Vidyarthi RS, Dwivedi DK (2016) Activating flux tungsten inert gas welding for enhanced weld penetration. *J Manuf Process* 22:211–228. <https://doi.org/10.1016/j.jmapro.2016.03.012>

33. Joseph J, Muthukumaran S (2017) Optimization of activated TIG welding parameters for improving weld joint strength of AISI 4135 PM steel by genetic algorithm and simulated annealing. *Int J Adv Manuf Technol* 93(1–4):23–34. <https://doi.org/10.1007/s00170-015-7599-8>
34. Chang YL, Lu L, Li YM, Yang X (2013) Forming mechanism of magnetic-controlled TIG high-speed welding seam. *Trans China Weld Inst* 34(06):1–4+113.
35. Ramkumar KD, Chandrasekar A, Singh AK, Ahuja S, Agarwal A, Arivazhagan N, Rabel AM (2016) Comparative studies on the weldability, microstructure and tensile properties of autogenous TIG welded AISI 430 ferritic stainless steel with and without flux. *J Manuf Process* 20:54–69. <https://doi.org/10.1016/j.jmapro.2015.09.008>
36. Vidyarthi RS, Dwivedi DK, Vasudevan M (2017) Influence of M-TIG and A-TIG welding process on microstructure and mechanical behavior of 409 ferritic stainless steel. *J of Materi Eng and Perform* 26(3):1391–1403. <https://doi.org/10.1007/s11665-017-2538-5>
37. Fan Y, Hong C, Huo YS (2018) Study on corrosion properties of A-TIG welded joints of 444 ultra pure ferritic stainless steel. *Modern Manufacturing Technology and Equipment* 05:23–24. <https://doi.org/10.16107/j.cnki.mmte.2018.0396>
38. Fei ZY, Pan ZX, Cuiuri D, Li HJ, Wu BT, Su LH (2019) Improving the weld microstructure and material properties of K-TIG welded armour steel joint using filler material. *Int J Adv Manuf Technol* 100:1931–1944. <https://doi.org/10.1007/s00170-018-2787-y>
39. Wu H, Chang YL, Mei Q, Liu D (2019) Research advances in high-energy TIG arc welding. *Int J Adv Manuf Technol* 104:391–410. <https://doi.org/10.1007/s00170-019-03918-5>
40. Xie Y, Cai YC, Zhang X, Luo Z (2018) Characterization of keyhole gas tungsten arc welded AISI 430 steel and joint performance optimization. *Int J Adv Manuf Technol* 99:347–361. <https://doi.org/10.1007/s00170-018-2257-6>
41. Yang MX, Zheng H, Qi BJ, Yang Z (2017) Effect of arc behavior on Ti-6Al-4V welds during high frequency pulsed arc welding. *J Mater Process Technol* 243:9–15. <https://doi.org/10.1016/j.jmatprotec.2016.12.003>
42. Hu SS, Han RF, Shen JQ, Han J, Xu HG (2013) Effect of pulse frequency on microstructure of 21% Cr ferritic stainless steel in pulsed gas tungsten arc welding. *Trans Tianjin Univ* 19:127–129. <https://doi.org/10.1007/s12209-013-1803-4>
43. Ramkumar KD, Mohan TH, Pandey R, Saxena V, Aravind S, Singh S (2016) Investigations on the structure-property relationships of PCGTA welds involving Inconel 718 and AISI 430. *Ciencia e Tecnologia dos Materiais* 29(2):28–38. <https://doi.org/10.1016/j.ctmat.2016.05.005>
44. Hu SS, Pang J, Shen JQ, Wu WY, Liu LL (2016) Microstructure, mechanical property and corrosion resistance property of Cr26Mo3.5 super ferritic stainless joints by P-TIG and laser welding. *Trans Tianjin Univ* 22:451–457
45. Qi BJ, Yang MX, Cong BQ, Liu FJ (2013) The effect of arc behavior on weld geometry by high-frequency pulse GTAW process with 0Cr18Ni9Ti stainless steel. *Int J Adv Manuf Technol* 66:1545–1553. <https://doi.org/10.1007/s00170-012-4438-z>
46. Nakada M, Shiohara Y, Flemings MC (1990) Modification of solidification structures by pulse electric discharging. *ISIJ Int* 30(1):27–33. <https://doi.org/10.2355/isijinternational.30.27>
47. Watanabe T, Shiroki M, Yanagisawa A, Sasaki T (2010) Improvement of mechanical properties of ferritic stainless steel weld metal by ultrasonic vibration. *J Mater Process Tech* 210(12):1646–1651. <https://doi.org/10.1016/j.jmatprotec.2010.05.015>
48. Lan HX, Gong XF, Zhang SF, Wang L, Wang B, Nie LP (2020) Ultrasonic vibration assisted tungsten inert gas welding of dissimilar metals 316L and L415. *Int J Miner Metall Mater* 27:943–953. <https://doi.org/10.1007/s12613-019-1960-0>
49. Chen C, Fan CL, Liu Z, Cai XY, Lin SB, Zhuo YM (2020) Microstructure evolutions and properties of Al–Cu alloy joint in the pulsed power ultrasonic-assisted GMAW. *Acta Metall Sin-Engl* 33:1397–1406. <https://doi.org/10.1007/s40195-020-01066-4>
50. Anttila S, Porter DA (2014) Influence of shielding gases on grain refinement in welds of stabilized 21 % Cr ferritic stainless steel. *Weld World* 58(6):805–817. <https://doi.org/10.1007/s40194-014-0160-9>
51. Zheng Y, Wang YC, Li H, Xing WQ, Yu XY, Dong P, Wang WX, Fan GW, Lian J, Ding M (2016) An experimental study of nitrogen gas influence on the 443 ferritic stainless steel joints by double-shielded welding. *Int J Adv Manuf Technol* 87:3315–3323. <https://doi.org/10.1007/s00170-016-8693-2>
52. Amuda MOH, Mridha S (2012) Grain refinement in medium chromium ferritic stainless steel welds via aluminum powder addition. *Advanced Materials Research* 445:717–722. <https://doi.org/10.4028/www.scientific.net/AMR.445.717>
53. Gurram M, Adepu K, Pinninti RR, Gankidi MR (2013) Effect of copper and aluminium addition on mechanical properties and corrosion behaviour of aisi 430 ferritic stainless steel gas tungsten arc welds. *J Mater Res Technol* 2(3):238–249. <https://doi.org/10.1016/j.jmrt.2013.02.009>
54. Parka LJ, Kong JP, Uhm SH, Woo IS, Lee JS, Kang CY (2011) Effect of Al–Si coating layer on the penetration and microstructures of ferritic stainless steel, 409L GTA welds. *J Mater Process Tech* 211:415–423. <https://doi.org/10.1016/j.jmatprotec.2010.10.017>
55. Kong JP, Park TJ, Kim JK, Uhm SH, Woo IS, Lee JS, Park BG, Kang CY (2011) Characterization of laser welds in Al-10 wt.%Si coated ferritic stainless steel. *Materials Design* 32(2):917–925. <https://doi.org/10.1016/j.matdes.2010.08.026>
56. Wu H, Chang YL, Lu L, Bai J (2017) Review on magnetically controlled arc welding process. *Int J Adv Manuf Technol* 91:4263–4273. <https://doi.org/10.1007/s00170-017-0068-9>
57. Li YW, Zou WF, Lee BY, Babkin A, Chang YL (2020) Research progress of aluminum alloy welding technology. *Int J Adv Manuf Technol* 109:1207–1218. <https://doi.org/10.1007/s00170-020-05606-1>
58. Wu H, Chang YL, Babkin A, Lee BY (2021) The behavior of TIG welding arc in a high-frequency axial magnetic field. *Weld World* 65:95–104. <https://doi.org/10.1007/s40194-020-01000-3>
59. Reddy GM, Meshram S (2006) Grain refinement in ferritic stainless steel welds through magnetic arc oscillation and its effect on tensile property. *Indian Weld J* 39:35–41. <https://doi.org/10.22486/iwj.v39i3.178461>
60. Ren P, Shi XC (2011) Analysis on the performance of 15Cr ferrite stainless steel and cracking of welded pipe. *Hot Working Technology* 40(13):166–168. <https://doi.org/10.14158/j.cnki.1001-3814.2011.13.068>
61. Meng YF, Ye B, Zhao D, Zhou K, Yu L, Qi XY (2017) Research on laser welding technology of 430 ferrite stainless steel strip fiber. *Applied laser* 37(01):79–84. <https://doi.org/10.14128/j.cnki.al.20173701.079>
62. Xu SF (2019) Laser welding process of ultra-pure ferritic stainless steel for elevator panels. *Welding technology* (5):62–64. <https://doi.org/10.13846/j.cnki.cn12-1070/tg.2019.05.018>
63. Lakshminarayanan AK, Balasubramanian V (2012) Evaluation of microstructure and mechanical properties of laser beam welded aisi 409m grade ferritic stainless steel. *J Iron Steel Res Int* 01:75–81. [https://doi.org/10.1016/S1006-706X\(12\)60050-8](https://doi.org/10.1016/S1006-706X(12)60050-8)
64. Liu LL, Hu SS, Shen JQ, Ma L, Wei X (2015) Effect of laser welding heat input on microstructure and properties of 26Cr-3.5Mo ferritic stainless steel. *Chin J Lasers* 42(02):101–107

65. Keskitalo M, Sundqvist J, Mäntyjärvi K, Powell J, Kaplan AFH (2015) The influence of shielding gas and heat input on the mechanical properties of laser welds in ferritic stainless steel. *Phys Procedia* 78:222–229. <https://doi.org/10.1016/j.phpro.2015.11.032>
66. Ma L, Hu SS, Hu B, Shen J, Wang YH (2014) Activating flux design for laser welding of ferritic stainless steel. *Trans Tianjin Univ* 20:429–434. <https://doi.org/10.1007/s12209-014-2243-5>
67. Elmesalamy A, Francis JA, Li L (2014) A comparison of residual stresses in multi pass narrow gap laser welds and gas-tungsten arc welds in AISI 316L stainless steel. *Int J Pres Ves Pip* 113:49–59. <https://doi.org/10.1016/j.ijpvp.2013.11.002>
68. Feng J, Guo W, Irvine N, Li L (2017) Understanding and elimination of process defects in narrow gap multi-pass fiber laser welding of ferritic steel sheets of 30 mm thickness. *Int J Adv Manuf Technol* 88:1821–1830. <https://doi.org/10.1007/s00170-016-8929-1>
69. Anh NV, Tashiro S, Hanh BV, Tanaka M (2018) Experimental investigation on the weld pool formation process in plasma key-hole arc welding. *Journal of Physics D: Applied Physics* 51(1). <https://doi.org/10.1088/1361-6463/aa9902>
70. Prasad KS, Damera CSR, NR, (2015) Application of grey relational analysis for optimizing weld bead geometry parameters of pulsed current micro plasma arc welded inconel 625 sheets. *Int J Adv Manuf Technol* 78:625–632. <https://doi.org/10.1007/s00170-014-6665-y>
71. Lakshminarayanan AK, Shanmugam V, Balasubramanian V (2009) Effect of autogenous arc welding processes on tensile and impact properties of ferritic stainless steel joints. *J Iron Steel Res Int* 16(1):62–68. [https://doi.org/10.1016/S1006-706X\(09\)60012-1](https://doi.org/10.1016/S1006-706X(09)60012-1)
72. KÖSE, C, Topal C (2019) Effect of post weld heat treatment and heat input on the microstructure and mechanical properties of plasma arc welded AISI 410S ferritic stainless steel. *Mater Res Express* 6(6). <https://doi.org/10.1088/2053-1591/ab09b6>
73. Hariharan SJ, Vigneshwar M, Selvamani ST, Shanmugam K, Palanikumar K (2019) Optimizing the plasma arc welding process parameters to attain the minimum corrosion rate in the AISI 409M grade ferritic stainless steel autogenous joints. *Materials Today: Proceedings* 16:1259–1270. <https://doi.org/10.1016/j.matpr.2019.05.223>
74. Zhu SC, Wang BS, Bi HY, Yan B (2018) Performance evaluation of 00Cr11NbTi perforated-plasma-arc-welded joint. *Baosteel Technical Research* 12(02):13–16
75. Li C, Wang BY (2018) Study on microstructure and corrosion resistance of 430 stainless steel micro-beam plasma arc welding joints. *Hot Working Technology* 47(07):34–37+41. <https://doi.org/10.14158/j.cnki.1001-3814.2018.07.008>
76. Siddaiah A, Singh BK, Mastanaiah P (2016) Prediction and optimization of weld bead geometry for electron beam welding of AISI 304 stainless steel. *Int J Adv Manuf Technol* 89(1):1–17. <https://doi.org/10.1007/s00170-016-9046-x>
77. Lakshminarayanan AK, Balasubramanian V, Reddy GM (2011) Microstructure and mechanical properties of electron beam-welded AISI 409M-grade ferritic stainless steel. *Int J Adv Manuf Technol* 55(1–4):153–162. <https://doi.org/10.1007/s00170-010-3044-1>
78. Lakshminarayanan AK, Balasubramanian V (2012) Influences of welding processes on microstructure and mechanical properties of modified 12 wt % Cr ferritic stainless steel. *Int J Manuf Res* 7(4):7679–7687. <https://doi.org/10.1504/IJMR.2012.050100>
79. Lakshminarayanan AK, Balasubramanian V, Reddy GM (2012) On the fatigue behaviour of electron beam and gas tungsten arc weldments of 409M grade ferritic stainless steel. *Mater Design* 35:760–769. <https://doi.org/10.1016/j.matdes.2011.10.010>
80. Balasubramanian V, Lakshminarayanan AK, Malarvizhi S (2013) Effect of welding processes on fatigue behaviour of AISI 409M grade ferritic stainless steel joints. *Advanced Materials Research* 794:391–412. <https://doi.org/10.4028/www.scientific.net/AMR.794.391>
81. Doomra A, Sandhu SS, Singh B (2020) Effect of post weld heat treatment on metallurgical and mechanical properties of electron beam welded AISI 409 ferritic steel. *Metallurgical and Materials Engineering* 26(3):279–292. <https://doi.org/10.30544/545>
82. Padhy GK, Wu CS, Gao S (2018) Friction stir based welding and processing technologies - processes, parameters, microstructures and applications: A review. *J Mater Sci Technol* 34(1):1–38. <https://doi.org/10.1016/j.jmst.2017.11.029>
83. Shah PH, Badheka VJ (2019) Friction stir welding of aluminium alloys: an overview of experimental findings - process, variables, development and applications. *Proceedings of the Institution of Mechanical Engineers. Part L Journal of Materials: Design and Application* 233(6): 1191–1226. <https://doi.org/10.1177/1464420716689588>
84. Patel V, Li W, Vairis A, Badheka V (2019) Recent development in friction stir processing as a solid-state grain refinement technique: microstructural evolution and property enhancement. *Critical Reviews in Solid State & Material Sciences* 44:378–426. <https://doi.org/10.1080/10408436.2018.1490251>
85. Lakshminarayanan AK, Balasubramanian V (2010) An assessment of microstructure, hardness, tensile and impact strength of friction stir welded ferritic stainless steel joints. *Mater Design* 31(10):4592–4600. <https://doi.org/10.1016/j.matdes.2010.05.049>
86. Lakshminarayanan AK, Balasubramanian V (2013) Process parameters optimisation for friction stir welding of aisi 409m grade ferritic stainless steel. *Exp Tech* 37(5):59–73. <https://doi.org/10.1111/j.1747-1567.2011.00802.x>
87. Salemi GA, Arab SM, Javadi F, Kargar F (2014) The effect of friction stir processing speed ratio on the microstructure and mechanical properties of a 430 ferritic stainless steel. *Journal of Advanced Materials and Processing* 2(2):39–48
88. Ahmed MMZ, Seleman ES, Shazly M, Attallah MM, Ahmed E (2019) Microstructural development and mechanical properties of friction stir welded ferritic stainless steel AISI 409. *J of Mater Eng and Perform* 28(5):1–16. <https://doi.org/10.1007/s11665-019-04365-9>
89. Sharma G, Dwivedi DK, Jain PK (2017) Characterization and strain-hardening behavior of friction stir-welded ferritic stainless steel. *J of Mater Eng and Perform* 26:5997–6005. <https://doi.org/10.1007/s11665-017-3020-0>
90. Mondal M, Das H, Ahn EY, Hong ST, Kim MJ, Han HN, Pal TK (2017) Characterization of friction stir welded joint of low nickel austenitic stainless steel and modified ferritic stainless steel. *Met Mater Int* 23(5):948–957. <https://doi.org/10.1007/s12540-017-6845-z>
91. Bilgin MB, Meran C, Canyurt OE (2014) Optimization of strength of friction stir welded joints for AISI 430 ferritic stainless steels by genetic algorithm. *Int J Adv Manuf Technol* 77(9–12):2221–2233. <https://doi.org/10.1007/s00170-014-6590-0>
92. Prakaash VGV, Vignesh A, Lakshminarayanan AK, Balasubramanian V (2015) Role of induction preheating on tool wear and properties of friction stir welded 409M stainless steel joints. *Appl Mech Mater* 787:401–405. <https://doi.org/10.4028/www.scientific.net/AMM.787.401>
93. Bina MH, Jamali M, Shamanian M, Sabet H (2015) Effect of welding time in the resistance spot welded dissimilar stainless steels. *Trans Indian Inst Met* 68:247–255. <https://doi.org/10.1007/s12666-014-0452-1>
94. Min D, Yong Z, Jie L (2016) Dissimilar spot welding joints of AZ31-443 ferritic stainless steel with cover plate. *Int J*

- Adv Manuf Technol 85:1539–1545. <https://doi.org/10.1007/s00170-015-8078-y>
95. Alizadeh-Sh M, Marashi SPH, Pouranvari M (2014) Resistance spot welding of AISI430 ferritic stainless steel: Phase transformations and mechanical properties. *Mater Design* 56:258–263. <https://doi.org/10.1016/j.matdes.2013.11.022>
 96. Subramanian A, Jabaraj DB, Raja VKB (2016) Mechanical properties and microstructure of resistance spot welded joints of AISI 409M ferritic stainless steel. *Trans Indian Inst Met* 69(3):767–774. <https://doi.org/10.1007/s12666-015-0551-7>
 97. Zhang Y, Guo J, Li Y, Luo Z, Zhang X (2020) A comparative study between the mechanical and microstructural properties of resistance spot welding joints among ferritic AISI 430 and austenitic AISI 304 stainless steel. *J Mater Res Technol* 9(1):574–583. <https://doi.org/10.1016/j.jmrt.2019.10.086>
 98. Ravichandran P, Anbu C, Meenakshipriya B, Sathiyavathi S (2020) Process parameter optimization and performance comparison of AISI 430 and AISI 1018 in resistance spot welding process. *Materials today: proceedings* 33(7):3389–3393. <https://doi.org/10.1016/j.matpr.2020.05.197>
 99. Sreehari M, Bhaskar GB (2018) Experimental investigations on resistance spot welding for producing indentation free joints on AISI 409m grade stainless steels. *Mater Res Express* 6(4). <https://doi.org/10.1088/2053-1591/aafa97>
 100. Onsekiz M, Altunpak Y (2017) Effect of electrode materials type on resistance spot welding of AISI 430 ferritic stainless steel. *Int J Eng Res Afr* 31:53–58. <https://doi.org/10.4028/www.scientific.net/JERA.31.53>
 101. Vishnuvaradhan K, Vignesh PV, Prabhu R (2017) Multi-response optimization of second pulse in resistance spot welding of ferritic stainless steel. *International Journal of Machine and Construction Engineering* 4(2)
 102. Deng F, Cao Q, Han X, Li L (2018) Electromagnetic pulse spot welding of aluminum to stainless steel sheets with a field shaper. *Int J Adv Manuf Technol* 98:1903–1911. <https://doi.org/10.1007/s00170-018-2208-2>
 103. Shan P, Yao Q, Li Y, Luo Z (2015) Reconstruction of current density distribution in weld area during resistance spot welding of aluminum alloy based on magnetic field. *Trans Tianjin Univ* 21:129–134. <https://doi.org/10.1007/s12209-015-2364-5>
 104. Min D, Wang YC (2016) Microstructure and properties evaluations of spot-welded ferritic steel sheets via static magnetic field. *Met Mater Int* 22(1):94–100. <https://doi.org/10.1007/s12540-015-5449-8>
 105. Wu CS, Zhang HT, Chen J (2017) Numerical simulation of key-hole behaviors and fluid dynamics in laser–gas metal arc hybrid welding of ferrite stainless steel plates. *J Manuf Process* 25:235–245. <https://doi.org/10.1016/j.jmapro.2016.11.009>
 106. Atabaki MM, Ma J, Yang G, Kovacevic R (2014) Hybrid laser/arc welding of advanced high strength steel in different butt joint configurations. *Mater Design* 64:573–587. <https://doi.org/10.1016/j.matdes.2014.08.011>
 107. Wahha M, Mizutani M, Katayama S (2016) Single pass hybrid laser-arc welding of 25 mm thick square groove butt joints. *Mater Design* 97:1–6. <https://doi.org/10.1016/j.matdes.2016.02.041>
 108. Zhang ZZ, Wu CS (2012) Monte Carlo simulation of grain growth in heat-affected zone of 12wt.% Cr ferritic stainless steel hybrid welds. *Comp Mater Sci* 65:442–449. <https://doi.org/10.1016/j.commatsci.2012.07.040>
 109. Zhang CY, Liu FC, Song ZX, Qian LH, Shen LJ, Zhou BS (2017) Influence of process parameters on grain size and mechanical properties of plasma and tig hybrid weld for 4003 ferritic stainless steel. *Hot working process* 046(7):42–46. <https://doi.org/10.14158/j.cnki.1001-3814.2017.07.012>
 110. Kim KH, Bang HS, Ro CS, Bang HS (2017) Influence of preheating source on mechanical properties and welding residual stress characteristics in ultra thin ferritic stainless steel hybrid friction stir welded joints. *Int J of Precis Eng and Manuf-Green Tech* 4(4):393–400. <https://doi.org/10.1007/s40684-017-0044-8>

Publisher's Note Springer Nature remains neutral with regard to jurisdictional claims in published maps and institutional affiliations.